



HAL
open science

HCV-Induced Epigenetic Changes Associated With Liver Cancer Risk Persist After Sustained Virologic Response

Nourdine Hamdane, Frank Jühling, Emilie Crouchet, Houssein El Saghire, Christine Thumann, Marine Oudot, Simonetta S. Bandiera, Antonio Saviano, Clara Ponsolles, Armando Andres Roca Suarez, et al.

► **To cite this version:**

Nourdine Hamdane, Frank Jühling, Emilie Crouchet, Houssein El Saghire, Christine Thumann, et al.. HCV-Induced Epigenetic Changes Associated With Liver Cancer Risk Persist After Sustained Virologic Response. *Gastroenterology*, 2019, 156 (8), pp.2313-2329.e7. 10.1053/j.gastro.2019.02.038 . inserm-02312806

HAL Id: inserm-02312806

<https://inserm.hal.science/inserm-02312806v1>

Submitted on 11 Oct 2019

HAL is a multi-disciplinary open access archive for the deposit and dissemination of scientific research documents, whether they are published or not. The documents may come from teaching and research institutions in France or abroad, or from public or private research centers.

L'archive ouverte pluridisciplinaire **HAL**, est destinée au dépôt et à la diffusion de documents scientifiques de niveau recherche, publiés ou non, émanant des établissements d'enseignement et de recherche français ou étrangers, des laboratoires publics ou privés.



Distributed under a Creative Commons Attribution - NonCommercial - NoDerivatives 4.0 International License

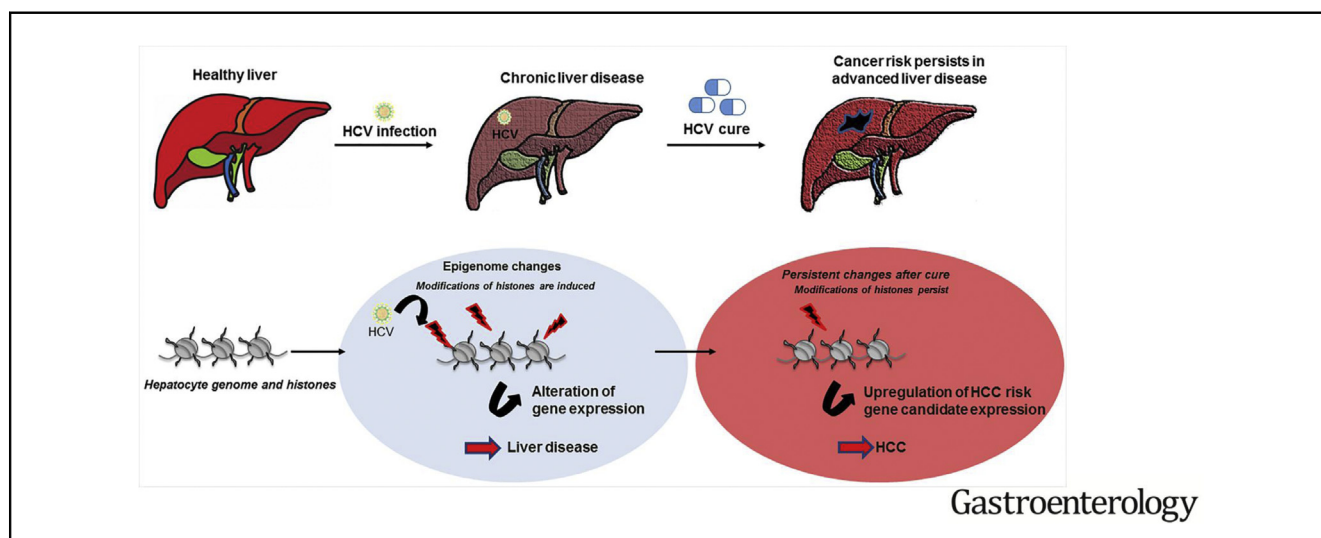
BASIC AND TRANSLATIONAL—LIVER

HCV-Induced Epigenetic Changes Associated With Liver Cancer Risk Persist After Sustained Virologic Response



Nourdine Hamdane,^{1,2,*} Frank Jühling,^{1,2,*} Emilie Crouchet,^{1,2} Houssein El Saghire,^{1,2} Christine Thumann,^{1,2} Marine A. Oudot,^{1,2} Simonetta Bandiera,^{1,2} Antonio Saviano,^{1,2,11} Clara Ponsolles,^{1,2} Armando Andres Roca Suarez,^{1,2} Shen Li,³ Naoto Fujiwara,⁴ Atsushi Ono,^{4,13,14} Irwin Davidson,⁵ Nabeel Bardeesy,⁶ Christian Schmid,^{7,8} Christoph Bock,^{7,9,10} Catherine Schuster,^{1,2} Joachim Lupberger,^{1,2} François Habersetzer,^{1,11} Michel Doffoël,¹¹ Tullio Piardi,¹² Daniele Sommacale,¹² Michio Imamura,¹³ Takuro Uchida,¹³ Hideki Ohdan,¹⁴ Hiroshi Aikata,¹³ Kazuaki Chayama,¹³ Tujana Boldanova,^{15,16} Patrick Pessaux,^{1,11} Bryan C. Fuchs,³ Yujin Hoshida,⁴ Mirjam B. Zeisel,^{1,2,17} François H. T. Duong,^{1,2,15} and Thomas F. Baumert^{1,2,11,18}

¹INSERM U1110, Institut de Recherche sur les Maladies Virales et Hépatiques, Strasbourg, France; ²Université de Strasbourg, Strasbourg, France; ³Division of Surgical Oncology, Massachusetts General Hospital Cancer Center, Harvard Medical School, Boston, Massachusetts; ⁴Liver Tumor Translational Research Program, Harold C. Simmons Comprehensive Cancer Center, Division of Digestive and Liver Diseases, University of Texas Southwestern Medical Center, Dallas, Texas; ⁵Department of Functional Genomics and Cancer, Institut de Génétique et de Biologie Moléculaire et Cellulaire, CNRS/INSERM/UDS, Illkirch, France; ⁶Center for Cancer Research, Massachusetts General Hospital; Departments of Medicine, Harvard Medical School, Boston, Massachusetts; ⁷CeMM Research Center for Molecular Medicine of the Austrian Academy of Sciences, Vienna, Austria; ⁸Regensburg Centre for Interventional Immunology (RCI) and University Medical Center of Regensburg, Regensburg, Germany; ⁹Department of Laboratory Medicine, Medical University of Vienna, Vienna, Austria; ¹⁰Max Planck Institute for Informatics, Saarbrücken, Germany; ¹¹Institut Hospitalo-Universitaire, Pôle Hépatite-digestif, Nouvel Hôpital Civil, Strasbourg, France; ¹²General, Digestive, and Endocrine Surgery Unit, Hôpital Robert Debré, Centre Hospitalier Universitaire de Reims, Université de Reims Champagne-Ardenne, Reims, France; ¹³Department of Gastroenterology and Metabolism, Applied Life Sciences, Institute of Biomedical & Health Sciences, Hiroshima University, Hiroshima, Japan; ¹⁴Department of Gastroenterological and Transplant Surgery, Graduate School of Biomedical and Health Sciences, Hiroshima University, Hiroshima, Japan; ¹⁵Department of Biomedicine, University Hospital Basel, University of Basel, Basel, Switzerland; ¹⁶Division of Gastroenterology and Hepatology, University Hospital Basel, University of Basel, Basel, Switzerland; ¹⁷INSERM U1052, CNRS UMR 5286, Cancer Research Center of Lyon (CRCL), Université de Lyon (UCBL), Lyon, France; and ¹⁸Institut Universitaire de France (IUF), Paris, France



See editorial on page 2130. See Covering the Cover synopsis on 2118.

BACKGROUND & AIMS: Chronic hepatitis C virus (HCV) infection is an important risk factor for hepatocellular

carcinoma (HCC). Despite effective antiviral therapies, the risk for HCC is decreased but not eliminated after a sustained virologic response (SVR) to direct-acting antiviral (DAA) agents, and the risk is higher in patients with advanced fibrosis. We investigated HCV-induced epigenetic alterations that might affect risk for HCC after DAA treatment in patients and mice

with humanized livers. **METHODS:** We performed genome-wide ChIPmentation-based ChIP-Seq and RNA-seq analyses of liver tissues from 6 patients without HCV infection (controls), 18 patients with chronic HCV infection, 8 patients with chronic HCV infection cured by DAA treatment, 13 patients with chronic HCV infection cured by interferon therapy, 4 patients with chronic hepatitis B virus infection, and 7 patients with nonalcoholic steatohepatitis in Europe and Japan. HCV-induced epigenetic modifications were mapped by comparative analyses with modifications associated with other liver disease etiologies. uPA/SCID mice were engrafted with human hepatocytes to create mice with humanized livers and given injections of HCV-infected serum samples from patients; mice were given DAAs to eradicate the virus. Pathways associated with HCC risk were identified by integrative pathway analyses and validated in analyses of paired HCC tissues from 8 patients with an SVR to DAA treatment of HCV infection. **RESULTS:** We found chronic HCV infection to induce specific genome-wide changes in H3K27ac, which correlated with changes in expression of mRNAs and proteins. These changes persisted after an SVR to DAAs or interferon-based therapies. Integrative pathway analyses of liver tissues from patients and mice with humanized livers demonstrated that HCV-induced epigenetic alterations were associated with liver cancer risk. Computational analyses associated increased expression of SPHK1 with HCC risk. We validated these findings in an independent cohort of patients with HCV-related cirrhosis ($n = 216$), a subset of which ($n = 21$) achieved viral clearance. **CONCLUSIONS:** In an analysis of liver tissues from patients with and without an SVR to DAA therapy, we identified epigenetic and gene expression alterations associated with risk for HCC. These alterations might be targeted to prevent liver cancer in patients treated for HCV infection.

Keywords: Biomarker; Biopsy; Chemoprevention; Sox9.

Chronic hepatitis C virus (HCV) infection is a leading cause of hepatocellular carcinoma (HCC), the second most common and fastest rising cause of cancer-related death.¹ The development of direct-acting antivirals (DAAs) with cure rates of higher than 90% has been a major breakthrough in the management of patients with chronic HCV infection. However, although viral cure decreases the overall HCC risk in HCV-infected patients, it does not eliminate virus-induced HCC risk, especially in patients with advanced fibrosis.^{2,3} Furthermore, convenient biomarkers to robustly predict HCC risk after viral cure and strategies for HCC prevention are absent.² These unexpected findings pose new challenges for patient management.⁴⁻⁶

Despite more than 2 decades of intensive research efforts, the pathogenesis of HCV-induced HCC and the HCC risk after DAA cure are still incompletely understood.^{6,7} Although HCV is an RNA virus with little potential for integrating its genetic material into the host genome, HCV contributes to hepatocarcinogenesis through a direct and an indirect way. HCV-mediated liver disease and carcinogenesis are considered multistep processes that include chronic infection-driven hepatic inflammation and progressive liver fibrogenesis with formation of neoplastic clones

WHAT YOU NEED TO KNOW

BACKGROUND AND CONTEXT

Despite effective antiviral therapies, the risk for HCC is not eliminated following a sustained virologic response to direct-acting antiviral (DAA) agents, and risk is higher in patients with advanced fibrosis.

NEW FINDINGS

In an analysis of liver tissues from patients with and without a sustained virologic response to DAA therapy, and from HCV-infected mice with humanized livers, the authors identified epigenetic and gene expression alterations associated with risk for HCC.

LIMITATIONS

This was a retrospective analysis of liver tissues from patients and mice.

IMPACT

The epigenetic alterations identified in this study might be targeted to prevent liver cancer in patients treated for HCV infection.

that arise and progress in the carcinogenic tissue microenvironment.^{4,6,8} A 186-gene expression signature in liver tissue of HCV-infected patients has been associated with HCC risk and mortality, suggesting that virus-induced transcriptional reprogramming in the liver could play a functional role in hepatocarcinogenesis.^{9,10}

Epigenetic modifications of histones can lead to chromatin opening and compacting and play a major role in gene regulation in health and disease.¹¹ Although epigenetic changes have been identified in established HCC,¹² their role in viral hepatocarcinogenesis remains largely unknown.


Methods

Human Subjects

Liver tissues from patients undergoing surgical resection or biopsy examination were collected at the Gastroenterology and Hepatology Clinic of the Hiroshima University Hospital (Hiroshima, Japan), the Basel University Hospital (Basel, Switzerland), the Centre Hospitalier Universitaire de Reims (Reims, France), and the Hôpitaux Universitaires de Strasbourg (Strasbourg, France). Protocols for patient tissue collection

*Authors share co-first authorship.

Abbreviations used in this paper: DAA, direct-acting antiviral; FC, fold change; GSEA, gene set enrichment analysis; HCC, hepatocellular carcinoma; HBV, hepatitis B virus; HCV, hepatitis C virus; IFN, interferon; mTOR, mammalian target of rapamycin; NASH, nonalcoholic steatohepatitis; PCA, principal component analysis; PLS, prognostic liver signature; SVR, sustained virologic response; TNF α , tumor necrosis factor α ; TSG, tumor suppressor gene.

 Most current article

© 2019 by the AGA Institute. Published by Elsevier Inc. This is an open access article under the CC BY-NC-ND license (<http://creativecommons.org/licenses/by-nc-nd/4.0/>).

0016-5085

<https://doi.org/10.1053/j.gastro.2019.02.038>

were reviewed and approved by the hospital ethics committees. Written and informed consent was obtained from all patients. Eligible patients were identified by a systematic review of patient charts. Histopathologic grading and staging of HCV liver biopsy specimens, according to the METAVIR classification system, were performed at the pathology institutes of the respective university hospitals. Overall, we analyzed liver tissue from 6 noninfected control patients, 18 patients with chronic HCV infection, 8 patients with DAA-cured chronic HCV, 13 patients with interferon (IFN)-cured chronic HCV, 4 patients with hepatitis B virus (HBV) infection, and 7 patients with nonalcoholic steatohepatitis (NASH). Furthermore, we studied 8 paired HCC samples with HCV-induced liver disease (Table 1).

HCV Infection of Human Hepatocyte Chimeric Mice and DAA Treatment

cDNA-uPA^{+/+}/SCID^{+/+} (uPA/SCID) mice were engrafted with human hepatocytes and intravenously inoculated with serum samples containing approximately 10⁵ HCV particles. HCV-infected mice were treated with a combination of MK-7009 and BMS-788329 DAAs.¹³ Elimination of HCV in treated mice was confirmed by the absence of HCV viremia 12 weeks after cessation of therapy. See the [Supplementary Materials](#) for further details.

ChIPmentation-Based ChIP-Seq

ChIPmentation-based ChIP-Seq on liver tissue using H3K27ac antibody (number 39134, Activ Motif, La Hulpe, Belgium) was performed as described previously¹⁴ and adapted as follows. To perform ChIP-Seq on human and mouse livers, tissues were cut in small pieces of 2–3 mm, crosslinked with 0.4% formaldehyde for 10 minutes at room temperature, and quenched with glycine 125 mmol/L for 5 minutes at room temperature. Then, tissue was homogenized using a glass potter and ChIPmentation was performed as described previously.¹⁴

Processing of Raw ChIPmentation Data

Reads were aligned to the human genome (hg19) and peaks were called in uniquely mapped reads using MACS2.⁸ Peaks within all samples were intersected and used for counting reads if they overlapped in at least 2 samples. Read counts of genes were defined as the sum of all reads in peak regions overlapping the gene body or the promoter region, that is, the region up to 1500 bp ahead of the transcription start site. See the [Supplementary Materials](#) for further details.

RNA Extraction and Next-Generation Sequencing

Liver tissues were lysed in TRI-reagent (Molecular Research Center; Cincinnati, OH) and RNA was purified using Direct-zol RNA MiniPrep (Zymo Research, Irvine, CA) or RNeasy kit (Qiagen, Hilden, Germany) according to the manufacturer's instructions. RNA quantity and quality were assessed using NanoDrop (Thermo Scientific, Waltham, MA) and Bioanalyzer 2100 (Illumina, San Diego, CA). Libraries of extracted RNA were prepared and sequenced as described previously.^{3,9}

Processing of RNA-Seq Data

Reads were counted with htseq-count, and a differentially expression analysis was performed with DESeq2 applying GENCODE 19.¹⁵ Reads were taken from our RNA-Seq experiments as described earlier and from external sources: RNA-Seq from infected (low ISG) vs control patients was retrieved from the GEO dataset GSE84346 (low ISG samples). See the [Supplementary Materials](#) for further details.

Pathway Enrichment and Correlation Analyses

Pathway enrichment analyses were performed using gene set enrichment analysis (GSEA) with all gene sets included in MSigDB 6.0.¹⁶ We used the pre-ranked version of GSEA and genes were ranked for *P* values of differential expression and modification analyses. Figures showing enriched pathways and gene sets, Spearman correlations, and oncogene log₂ fold change (FC) were drawn using ggplot2 and the R environment (R Foundation, Vienna, Austria). Gene network analysis was performed based on 3 MSigDB subsets: Hallmark gene sets, curated gene sets, and gene ontology gene sets. See the [Supplementary Materials](#) for further details.

Western Blot

Expression of SPHK1 and SOX9 proteins was assessed by western blot and quantified using ImageJ software (National Institutes of Health, Bethesda, MD). See the [Supplementary Materials](#) for further details.

Association of Hepatic Gene Expression With Prognostic Cox Score for Overall Death

Prognostic association of hepatic gene expression was determined using the Cox score for time to overall death in HCV-infected patients with advanced liver disease and HCC as previously described.¹⁷

Gene Expression and Assessment of HCC Risk in HCV Cohorts

Patients with early-stage HCV cirrhosis (*n* = 216¹⁰; GSE15654) and a subgroup of patients who had achieved a sustained virologic response (SVR) before the biopsy (*n* = 21) were classified into SPHK1-high and -low expression groups based on the cutoff value of 1 sample standard deviation above the mean. Cumulative probabilities of HCC development were calculated using the Kaplan-Meier procedure and compared by log-rank test.

Data Availability

The Sequence Read Archive accession number for the data reported in this study is SRP170244.

Results

Virus-Induced Modifications of Histone Mark H3K27ac Persist in Human Liver After DAA Cure in HCV-Infected Patients

To investigate whether chronic HCV infection triggers persistent epigenetic modifications after cure, we performed a genome-wide analysis using ChIPmentation-based

Table 1. Characteristics of Studied Patients

	Biopsy ID	Sex	Age	Diagnosis	Viral genotype	Viral load (IU/mL)	METAVIR grade	METAVIR stage	Antiviral treatment
Controls	C1	F	55	Minimal hepatitis	N/A	N/A	N/A	F0	N/A
	C2	M	46	Minimal hepatitis	N/A	N/A	N/A	F0	N/A
	C3	F	40	Lobular hepatitis	N/A	N/A	N/A	F0	N/A
	C4	F	53	Minimal hepatitis	N/A	N/A	N/A	F0	N/A
	C5	M	56	Lobular hepatitis	N/A	N/A	N/A	F0	N/A
	C6	F	58	Minimal hepatitis	N/A	N/A	N/A	F0	N/A
	C7	F	51	Chronic indeterminate hepatitis	N/A	N/A	N/A	F3	N/A
	C8	F	37	Acute partially cholestatic hepatitis	N/A	N/A	N/A	F0	N/A
	C9	F	44	Cholestatic hepatitis	N/A	N/A	N/A	F1	N/A
	C10	M	78	Adjacent liver from CCM resection	N/A	N/A	N/A	N/A	N/A
	C11	F	58	Adjacent liver from CCM resection	N/A	N/A	N/A	N/A	N/A
	C12	F	70	Adjacent liver from CCM resection	N/A	N/A	N/A	N/A	N/A
	C13	M	63	Adjacent liver from CCM resection	N/A	N/A	N/A	N/A	N/A
	C14	M	70	Adjacent liver from CCM resection	N/A	N/A	N/A	N/A	N/A
	C15	F	69	Adjacent liver from CCM resection	N/A	N/A	N/A	N/A	N/A
	C16	M	53	Adjacent liver from CCM resection	N/A	N/A	N/A	N/A	N/A
	C17	M	71	Adjacent liver from CCM resection	N/A	N/A	N/A	N/A	N/A
HBV	B1	F	46	HBV	N/A	N/A	N/A	F4	NUC
	B2	M	65	HBV and HCC	N/A	N/A	N/A	F4	NUC
	B3	M	57	HBV and HCC	N/A	N/A	N/A	F4	NUC
	B4	M	58	HBV and HCC	N/A	N/A	N/A	F4	NUC
NASH	N1	M	27	NASH and HCC	N/A	N/A	N/A	F4	N/A
	N2	M	63	NASH and HCC	N/A	N/A	N/A	F4	N/A
	N3	M	73	NASH and HCC	N/A	N/A	N/A	F4	N/A
	N4	M	76	NASH and HCC	N/A	N/A	N/A	F4	N/A
	N5	F	65	NASH and HCC	N/A	N/A	N/A	F4	N/A
	N6	F	47	NASH and HCC	N/A	N/A	N/A	F4	N/A
	N7	F	68	NASH and HCC	N/A	N/A	N/A	F4	N/A
HCV infected	H1	F	62	Chronic HCV	1a	5140000	A1	F1	Naïve
	H2	M	44	Chronic HCV	1a	7.41E + 06	A1	F2	Naïve
	H3	F	23	Chronic HCV	3a	2.46E + 02	A2	F2	Naïve
	H4	F	60	Chronic HCV	2	2.70E + 06	A2	F2	Naïve
	H5	M	23	Chronic HCV	1a	1.76E + 06	A1	F1	Intolerant to Peg-IFN/RBV
	H6	M	48	Chronic HCV	1a	5.93E + 06	A1	F2	Naïve
	H7	F	38	Chronic HCV	1b	7.95E + 05	A1	F2	Naïve
	H8	M	58	Chronic HCV	4	4.08E + 06	A3	F2	Nonresponder to Peg-IFN/RBV
	H9	M	52	Chronic HCV	1a	6.60E + 05	A3	F3	Naïve
	H10	M	54	Chronic HCV and HCC	1b	4.40E + 04	A1	F4	Relapse to SOF/DCV/RBV
	H11	M	68	Chronic HCV and HCC	2a	2.51E + 05	A3	F3	Naïve

Table 1. Continued

	Biopsy ID	Sex	Age	Diagnosis	Viral genotype	Viral load (IU/mL)	METAVIR grade	METAVIR stage	Antiviral treatment
	H12	M	51	Chronic HCV	3a	3.30E + 06	A2	F1	Naïve
	H13	M	54	Chronic HCV	4	3.31E + 06	A2	F1	Naïve
	H14	F	48	Chronic HCV	3a	1.15E + 06	A3	F4	Naïve
	H15	M	65	Chronic HCV	1b	2.25E + 06	A2	F4	Naïve
	H16	M	81	Chronic HCV and HCC	1b	1.85E + 06	A1	F1	Nonresponder to Peg-IFN/RBV
	H17	M	51	Chronic HCV and HCC	3a	3.79E + 06	A2	F4	Relapse to SOF/RBV
	H18	F	71	Chronic HCV and HCC	1b	3.93E + 06	A1	F1	Naïve
	H19	F	49	Chronic HCV	3a	3.50E + 06	A3	F4	Naïve
	H20	M	34	Chronic HCV	N/A	2.21E + 06	A3	F4	Naïve
	H21	M	53	Chronic HCV	1	1.35E + 06	A3	F4	Naïve
	H22	F	62	Chronic HCV	N/A	6.10E + 06	A3	F4	Naïve
	H23	F	59	Chronic HCV	4	2.68E + 06	A3	F4	Naïve
	H24 ^a	M	79	Chronic HCV and HCC	1b	2.00E + 06	A2	F2	N/A
	H25 ^a	M	56	Chronic HCV and HCC	1b	2.00E + 06	A3	F4	N/A
	H26 ^a	F	79	Chronic HCV and HCC	1b	5.01E + 05	A2	F4	N/A
	H27 ^a	M	85	Chronic HCV and HCC	1b	3.16E + 05	A3	F3	N/A
	H28 ^a	M	64	Chronic HCV and HCC	2b	1.00E + 07	A2	F4	N/A
	H29 ^a	F	76	Chronic HCV and HCC	1b	6.31E + 06	A2	F4	N/A
	H30 ^a	F	84	Chronic HCV and HCC	1b	5.01E + 04	A2	F3	N/A
	H31 ^a	M	61	Chronic HCV and HCC	1b	3.98E + 04	A2	F2	N/A
HCV cured	D1 ^a	M	65	Cured HCV and HCC	1b	Undetectable	A0	F2	SOF/DCV
	D2 ^a	M	58	Cured HCV and HCC	1a	Undetectable	A0	F4	SOF/LDV
	D3 ^a	F	79	Cured HCV and HCC	1b	Undetectable	A2	F4	DCV/ASV
	D4 ^a	M	63	Cured HCV and HCC	2a	Undetectable	A2	F4	SOF/RBV
	D5 ^a	M	69	Cured HCV and HCC	1b	Undetectable	A2	F3	DCV/ASV
	D6 ^a	M	73	Cured HCV and HCC	1b	Undetectable	A2	F3	DCV/ASV
	D7 ^a	M	75	Cured HCV and HCC	1b	Undetectable	A2	F3	SOF/LDV
	D8 ^a	F	75	Cured HCV and HCC	1b	Undetectable	A2	F3	SOF/LDV
	D9 ^a	M	71	Cured HCV and HCC	1B	Undetectable	A3	F2	DCV/ASV
	D10 ^a	M	73	Cured HCV and HCC	1B	Undetectable	A2	F3	DCV/ASV
	D11 ^a	F	76	Cured HCV and HCC	1B	Undetectable	A2	F2	DCV/ASV
	D12 ^a	M	61	Cured HCV and HCC	2A	Undetectable	A2	F3	SOF/RBV
	D13 ^a	F	71	Cured HCV and HCC	1B	Undetectable	A2	F4	DCV/ASV
	D14 ^a	M	79	Cured HCV and HCC	1B	Undetectable	N/A	N/A	DCV/ASV
	D15 ^a	M	64	Cured HCV and HCC	1B	Undetectable	A2	F3	SOF/LDV
	D16 ^a	M	78	Cured HCV and HCC	1B	Undetectable	A1	F1	SOF/LDV
	I1	M	68	Cured HCV and HCC	2A	Undetectable	N/A	F3	Peg-IFN/RBV
	I2	M	61	Cured HCV and HCC	2A	Undetectable	A2	F4	Peg-IFN/RBV
	I3	F	74	Cured HCV and HCC	2B	Undetectable	A2	F3	IFN/RBV
	I4	M	69	Cured HCV and HCC	1B	Undetectable	A1	F2	Peg-IFN/RBV
	I5	M	66	Cured HCV and HCC	2B	Undetectable	A2	F4	IFN

Table 1. Continued

Biopsy ID	Sex	Age	Diagnosis	Viral			Antiviral treatment
				genotype	load (IU/mL)	METAVIR grade	
16	F	68	Cured HCV and HCC	1B	Undetectable	A2	IFN
17	M	54	Cured HCV and HCC	1B	Undetectable	A2	Peg-IFN/RBV
18	M	66	Cured HCV and HCC	1B	Undetectable	A1	IFN
19	M	74	Cured HCV and HCC	2A	Undetectable	A2	Peg-IFN
110	M	80	Cured HCV and HCC	1B	Undetectable	A1	Peg-IFN/RBV
111	F	77	Cured HCV and HCC	1B	Undetectable	A1	Peg-IFN/RBV
112	M	70	Cured HCV and HCC	1B	Undetectable	A1	Peg-IFN
113	M	65	Cured HCV and HCC	1B	Undetectable	A2	Peg-IFN/RBV

NOTE. Biopsy identification number, sex, age, pathologic diagnosis, HCV genotype and load, antiviral treatment (for HCV-infected and HCV-cured patients), and METAVIR grade (when applicable) and score are presented.

ASV, asunaprevir; CCM, colon cancer metastasis; DCV, daclatasvir; F, female; IU, international unit; LDV, ledipasvir; M, male; N/A, not applicable; NUC, nucleos(t)ide analogues; Peg, pegylated; RBV, ribavirin; SOF, sofosbuvir.

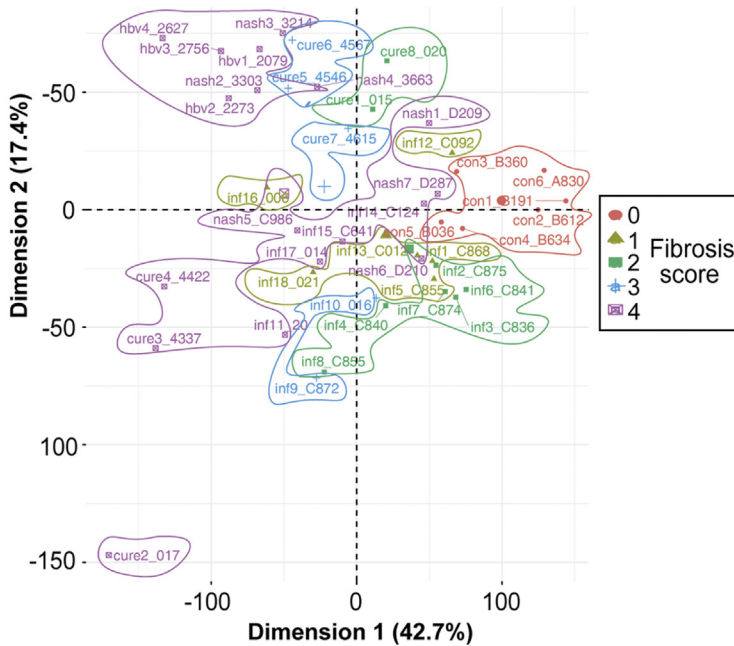
^aPaired analysis of HCC and nontumor tissue.

ChIP-Seq¹⁴ profiling the well-characterized histone modification H3K27ac in liver tissues from 18 patients with chronic HCV infection, 21 patients with DAA- or IFN-based curative therapy, and 6 noninfected controls (Figure 1A and Table 1). The H3K27ac modification is associated with active promoters and enhancers and with activation of transcription.¹⁸ We observed significant changes in specific H3K27ac modifications in HCV-infected patients compared with noninfected controls (Figures 1B and Supplementary Figure 1). To study whether these were etiology specific, we performed comparative analyses of liver tissues with chronic HCV infection (n = 18), chronic HBV infection (n = 4), and NASH (n = 7). Using principal component analysis (PCA), we found that the distribution of H3K27ac changes in the epigenome of livers of noninfected, HCV-infected, HBV-infected, and NASH samples formed distinct clusters on the PCA plot, suggesting that an important part of the changes are etiology specific (Figure 2A). Next, we performed a correlation analysis of H3K27ac changes among HCV-infected, HBV-infected, and NASH samples. Our data showed a positive correlation of H3K27ac changes (Figure 2B) among patients with NASH ($r = 0.83$; $P < 10^{-10}$), or patients with HBV infection ($r = 0.79$; $P < 10^{-10}$), or HCV infection, suggesting that some epigenetic modifications are shared among etiologies. To analyze the impact of epigenetic changes in genes related to immune responses, we extracted immune-related genes from MSigDB and performed a restricted correlation study that showed lower correlation coefficients (NASH vs HCV, $r = 0.75$, $P < 10^{-10}$; HBV vs HCV, $r = 0.62$, $P < 10^{-10}$) compared with analyses composed of all genes (Supplementary Figure 2). These findings suggest that epigenetic modifications in immune genes associated with inflammatory responses are only partly responsible for the similarities between etiologies.

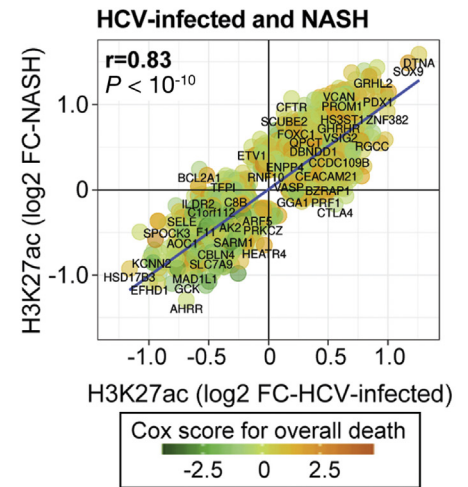
Recent studies have reported a correlation between fibrosis and an increased incidence of HCC.⁶ However, the molecular mechanism of fibrosis-induced HCC is not well understood. Our comparative analysis showed that H3K27ac modifications, separated based on fibrosis score along the primary component (dimension 1), accounted for 42% of the variation between samples. This suggests that a substantial fraction of the observed H3K27ac alterations is related to liver fibrosis. Interestingly, we did not observe any significant correlation between these epigenetic changes and the activity score (ie, reflecting liver inflammation), suggesting that aberrant H3K27 acetylation is less dependent of necro-inflammatory activity but rather dependent on the fibrosis stage (Figure 1B).

By comparing H3K27ac modifications in liver tissue with chronic HCV infection before DAA treatment and in liver tissue with successful DAA cure, we studied whether epigenetic changes persisted in cured patients. Interestingly, we found a significant and positive correlation of H3K27ac modifications after comparing HCV-infected and DAA-cured samples ($r = 0.87$; $P < 10^{-10}$; Figure 2C). A comparative analysis showed a strong positive correlation between epigenetic changes in liver samples of DAA-cured and IFN-cured patients ($r = 0.91$; $P < 10^{-10}$; Supplementary Figure 1B), suggesting that HCV-

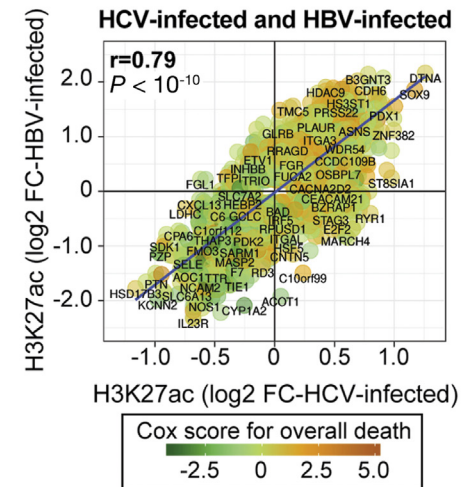
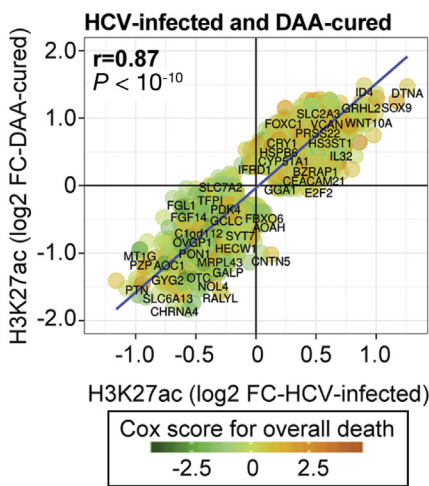
A



B

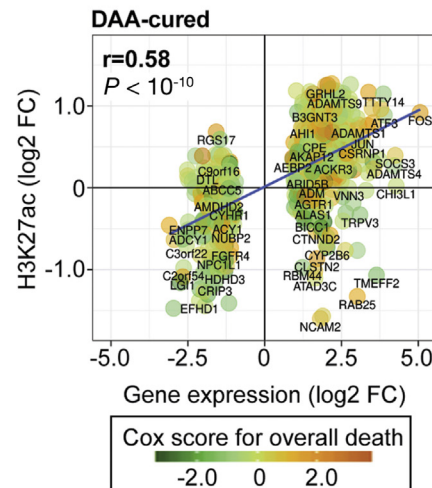
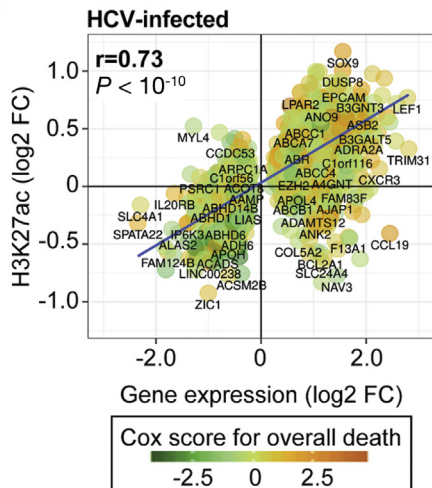


C



BASIC AND TRANSLATIONAL LIVER

D



Persistent Epigenetic Changes Are Associated With Liver Carcinogenesis After Cure

Epigenetic regulation is an indispensable process for normal development and preservation of tissue-specific gene expression profiles. Thus, any perturbation in the epigenetic landscape can lead to shifted gene function and malignant cellular transformation. We addressed the potential functional role of the observed alterations for virus-induced liver disease and hepatocarcinogenesis by performing a pathway enrichment analysis of genes associated with H3K27ac changes in liver tissues from HCV-infected and cured patients. We found that chronic HCV infection induces significant epigenetic H3K27ac changes on genes that belong to pathways related to tumor necrosis factor α (TNF α), inflammatory response, and interleukin 2 and signal transducer and activator of transcription 5 signaling (Figure 3A). Furthermore, we observed lower levels of H3K27ac within genes related to pathways associated with coagulation and metabolism, such as oxidative phosphorylation, fatty acid metabolism, or adipogenesis (Figure 3A). Remarkably, several altered pathways persisted after cure (eg, TNF α signaling, inflammatory response, G2M checkpoint, epithelial–mesenchymal transition, and phosphoinositide 3-kinase, Akt, and mammalian target of rapamycin [mTOR]; Figure 3A). We also observed lower levels of H3K27ac mapping to genes related to oxidative phosphorylation pathways (Figure 3A). Overall, our data provide evidence supporting a functional role for H3K27ac changes in establishing gene expression patterns that persist after cure and contribute to carcinogenesis.

We proceeded to study the impact of fibrosis on persistence of epigenetic modifications. Our analysis showed that H3K27ac changes observed in HCV-infected patients were partly reversed in cured patients with stage F2–3 fibrosis. This group shared 2259 of the 5318 (42.5%) modified genes in the HCV-infected group (Figure 3B). In contrast, in DAA-cured patients with advanced liver disease (F4), the HCV-induced H3K27ac changes largely persisted. The HCV-infected group shared nearly all modified genes (96.6%, 5140 of 5318 genes) with F4 cured patients (Figure 3B). Collectively, we identified significant changes of H3K27ac levels on 2193 genes persisting in the 2 DAA-cured patient groups (Figure 3B and Supplementary Table 1). Among these candidates, we identified oncogenes and tumor suppressor genes (TSGs) that are associated with, respectively, increased or decreased levels of H3K27ac (Figure 3C). These alterations were even more pronounced in patients with

advanced fibrosis (Figure 3C), correlating with an enhanced risk for developing HCC in F4 vs F2–F3.^{2,3} Importantly, we found a clear correlation between transcriptomic and epigenomic changes of the identified oncogenes and TSGs, supporting the biological relevance of the findings (Figure 3D). Among these oncogenes was *SPHK1*, a lipid kinase mediating the phosphorylation of sphingosine to form SP1, which is a major regulator of cell apoptosis inhibition and proliferation promotion. *SPHK1* and *SP1* play key roles in the TNF α and nuclear factor κ B signaling pathways.¹⁹ *SPHK1* expression is increased and associated with tumor size and progression in patients with HCC.²⁰ Among the TSGs with significantly decreased H3K27ac level in HCV-infected patient livers were *PTPRD*, *TSC2*, and the major regulator of DNA repair, *BRCA1*. *PTPRD* has been identified as a candidate tumor suppressor in the liver impaired by HCV infection.²¹ *TSC2* has been reported to be a negative regulator of the mTOR signaling pathway. Its down-regulation is associated with metabolic defects, liver disease progression, and carcinogenesis.⁷ Collectively, the overexpressed oncogenes and down-regulated TSGs that are enriched or decreased for the H3K27ac mark in chronic HCV infection, respectively, are involved in processes that favor carcinogenesis.

To further confirm that the persistent H3K27ac changes are linked to HCC risk, we referred to the genes of the recently reported 186-gene prognostic liver signature (PLS) and a 32-gene subset thereof for predicting liver disease progression, HCC development, and death for all HCC etiologies.^{9,17,22} We analyzed functional links, that is, commonly shared pathways in MsigDB, among the 32-gene set, the 2193 genes with persistent epigenetic and transcriptional modifications, and the hallmarks of cancer.²³ We found that 1411 of the identified genes are closely connected to the PLS through shared pathways. Then, we assigned categories related to the hallmarks of cancer to the deregulated genes to understand the pathophysiologic impact of chronic HCV infection. Our analyses showed that approximately 900 genes of the genes with epigenetic modifications are directly linked with carcinogenesis. A network of these genes associated with at least 1 hallmark of cancer is shown in Figure 3E.

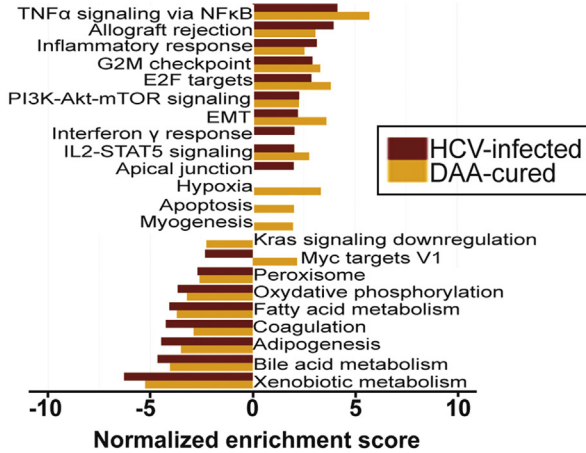
Next, we investigated whether H3K27ac alterations persist in cancer tissues after cure. We performed pairwise comparison of HCC and adjacent nontumorous tissue from the individual DAA-treated patient. We found a genome-wide H3K27ac enrichment in adjacent nontumorous and in tumorous tissues compared with noninfected samples (Figure 4). Deeper analysis showed that 52% of H3K27ac enriched genes are specific to tumorous tissues, 31% are

Figure 2. HCV-infection induces specific epigenetic changes in the liver of HCV-infected patients. (A) PCA for control, noninfected, HCV-infected, DAA-cured, IFN-cured, HBV-infected, and NASH patient samples. Comparative analysis of epigenetic modifications separated based on fibrosis score along the primary component (dimension 1). (B) H3K27ac modifications among HCV-infected patients correlate (Spearman rank correlation coefficients and *P* values) with H3K27ac modifications among NASH or HBV-infected patients. Common H3K27ac modifications were analyzed. Prognostic association of hepatic gene expression was determined by using Cox score for time to overall death in a cohort of patients as previously described.¹⁷ (C) HCV-induced and persistent epigenetic changes after DAA cure in patient-derived liver tissue are associated with a decreased survival and death. H3K27ac modifications among HCV-infected correlate with persistent H3K27ac modifications among DAA-cured patients. (D) H3K27ac modifications correlate with significantly differentially expressed genes in HCV-infected and DAA-cured patients.

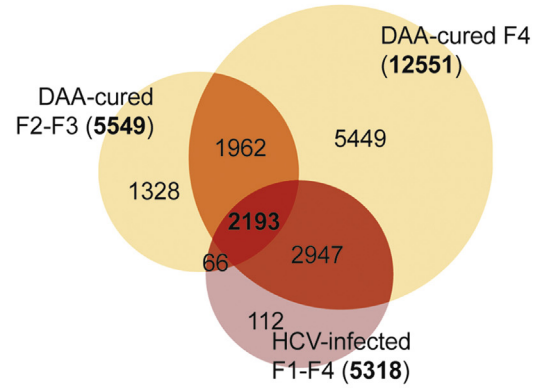
specific to adjacent nontumorous tissues, and 17% are common to the paired tissue. These data suggest that epigenetic alterations persist from advanced fibrosis to HCC and therefore could play a pathogenic role in

hepatocarcinogenesis before and after cure. Furthermore, the presence of epigenetic modifications in adjacent tumor tissue suggests that the epigenetic modifications might precede hepatocarcinogenesis.

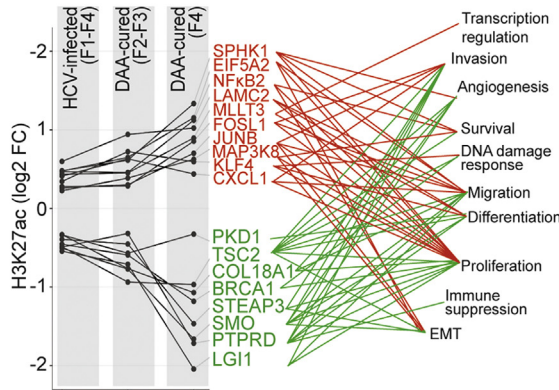
A



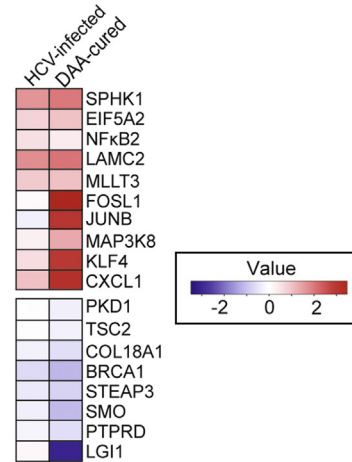
B



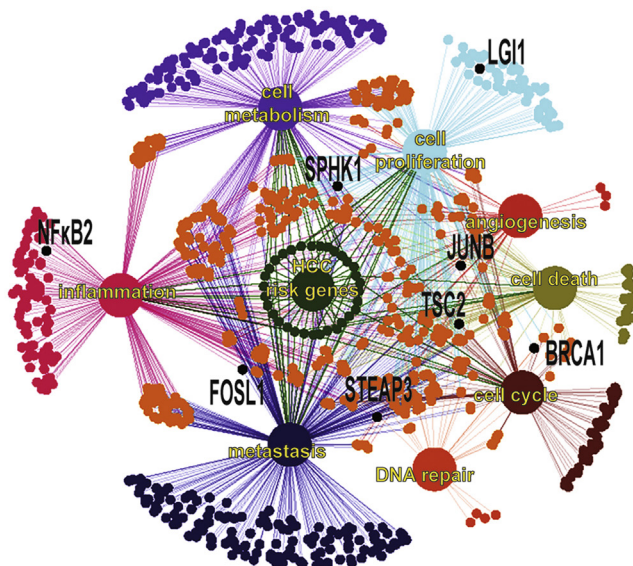
C



D



E



Hallmarks of cancer

- HCC risk genes
- Metastasis-associated genes
- Inflammation-associated genes
- Angiogenesis-associated genes
- Cell death-associated genes
- Cell cycle-associated genes
- DNA repair-associated genes
- Cell proliferation-associated genes
- Cell metabolism-associated genes
- Shared genes

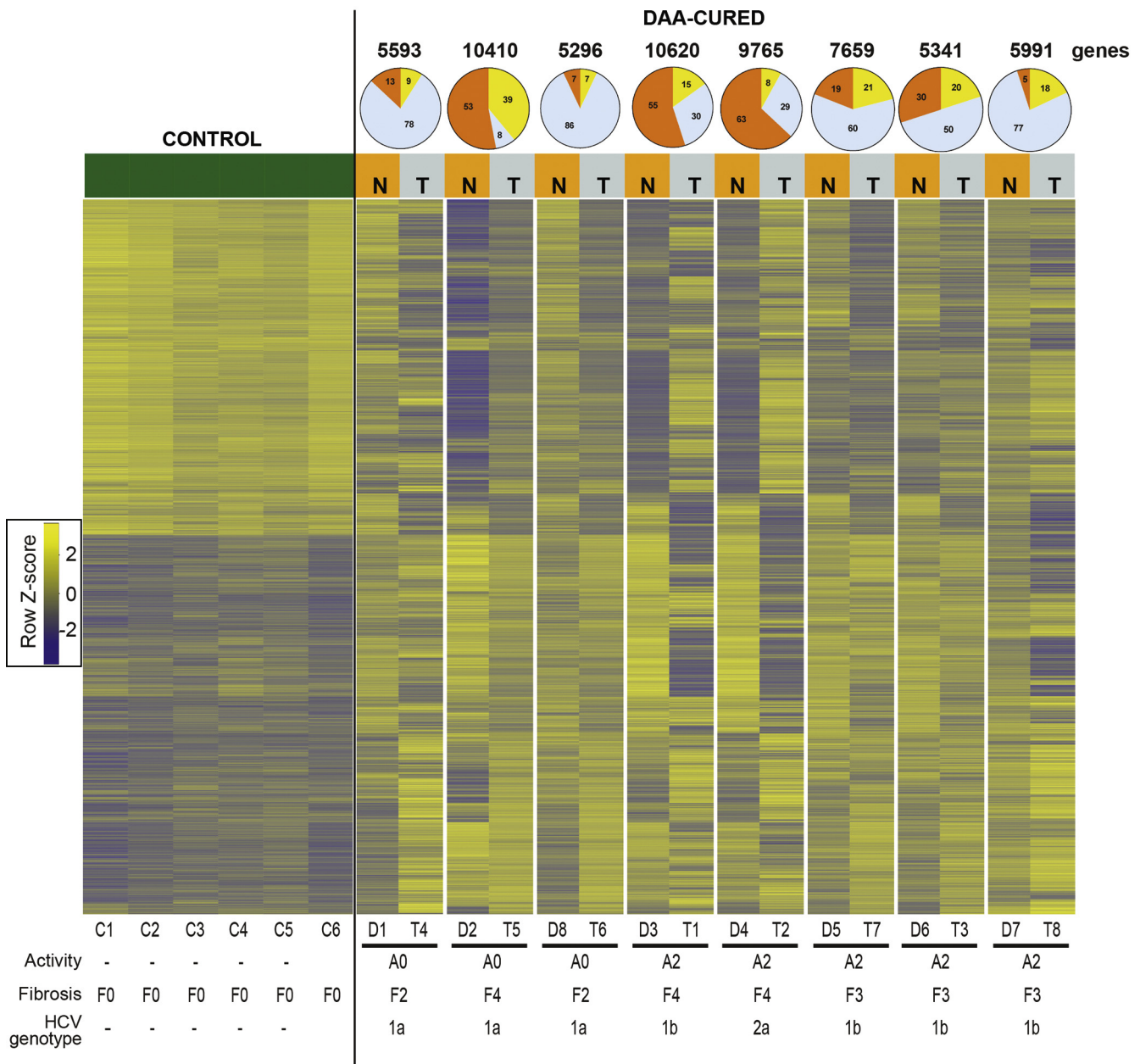
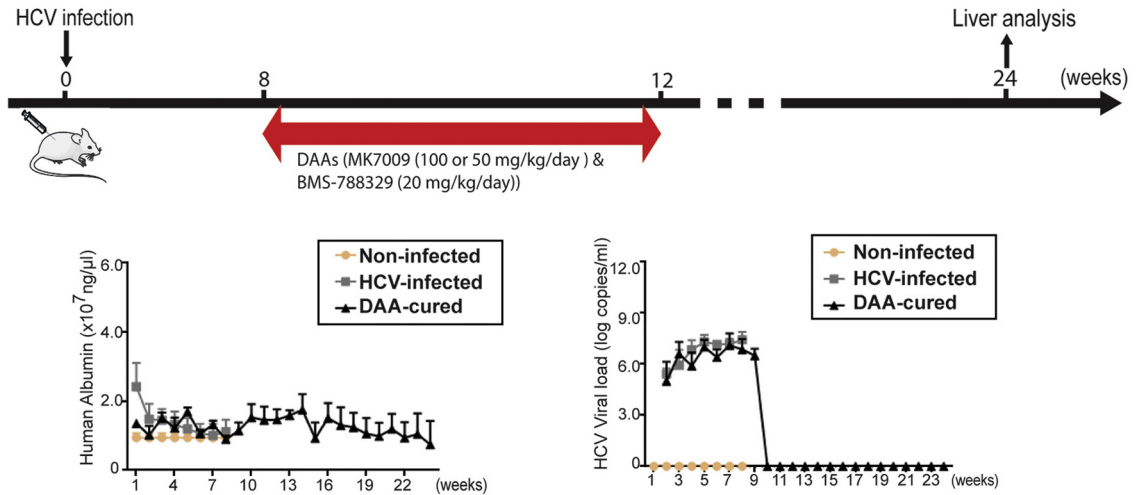


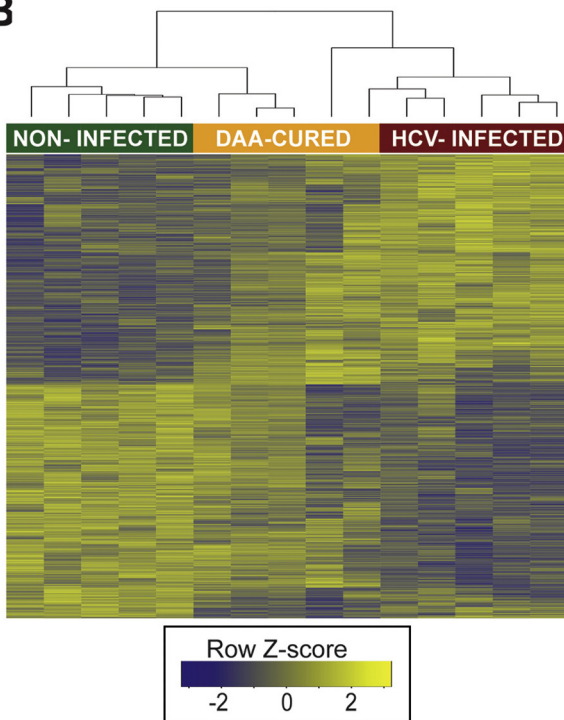
Figure 4. HCV-induced epigenetic changes persisting after DAA-based cure are present in the tumor tissue of patients with DAA-cured HCC. H3K27ac modifications from patient-derived resections of tumor and nontumor adjacent paired tissue samples. Similar to the analysis shown in Figure 1B, we performed an unsupervised clustering of normalized read counts in ChIP-Seq peaks of 7609 genes linked with significant ($q < 0.05$) H3K27ac modifications in DAA-cured adjacent ($n = 8$) or paired-tumor ($n = 8$) tissues vs noninfected control patients ($n = 6$). The proportions (percentages) of common (yellow) or distinct genes associated with changes in H3K27ac levels in tumor (blue) or nontumor paired-adjacent tissues (orange) are represented as a pie chart. N, nontumor; T, tumor.

Figure 3. Pathway analysis of epigenetic and transcriptional reprogramming in HCV-infected patients unravels candidate genes driving carcinogenesis after DAA cure. (A) Hallmark pathways significantly enriched for H3K27ac modifications in infected ($n = 18$) or/and DAA-cured ($n = 8$) compared with control ($n = 6$) patient samples. A large overlap of enriched pathways persists in DAA-cured patients. (B) Venn diagram showing HCC risk gene candidates as the overlap of significantly modified genes in HCV-infected (F1–F4) and DAA-cured (F2–F3 and F4) patients derived from the ChIP-Seq experiment shown in Figure 1B. (C) Oncogenes (red) and TSGs (green) from the 2193 potential HCC risk gene candidates, with their biological functions indicated. (D) Heat map depicting transcriptional changes of the oncogenes and TSGs described in C in HCV-infected and DAA-cured patients. (E) Genes with persistent HCV-induced H3K27ac modifications after DAA cure, linked with the 32-gene prognostic liver signature predicting HCC in HCV-infected patients,^{9,17} and overlapped with the hallmarks of cancer. Oncogenes shown in D are highlighted in black. This network includes 910 potential HCC risk gene candidates, highlighting a strong enrichment for modifications linked to carcinogenesis. EMT, epithelial–mesenchymal transition; IL2, interleukin 2; PI3K, phosphoinositide 3-kinase; STAT5, signal transducer and activator of transcription 5.

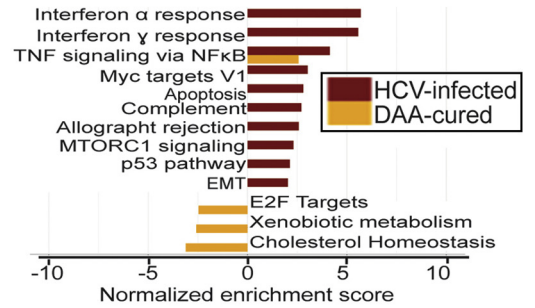
A



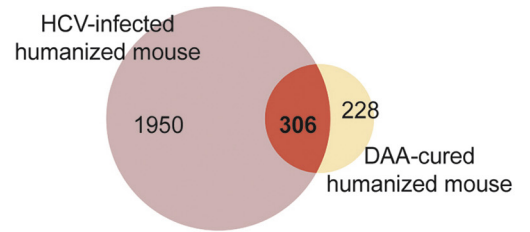
B



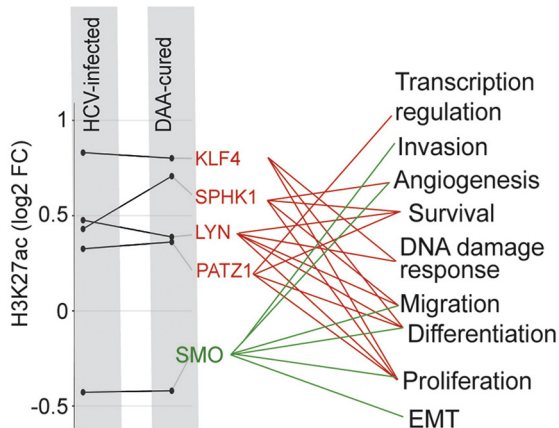
C



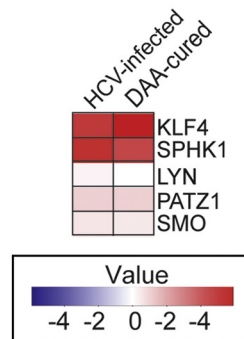
D



E



F



Identification of HCV-Specific Epigenetic and Transcriptional Modifications That Are Independent of Inflammation and Fibrosis Using a Human Liver Chimeric Mouse Model

In the HCV-infected patient livers, epigenetic and transcriptional changes are most likely due to direct HCV-hepatocyte interactions and indirect mechanisms caused by chronic inflammation and fibrosis. Furthermore, our analysis is based on bulk tissue in which hepatocyte-related changes are difficult to distinguish from those in non-parenchymal cells. To clarify which fraction of the observed changes is dependent on HCV-hepatocyte interactions, we applied an HCV-permissive human liver chimeric mouse model.¹³ In this model HCV efficiently infects the engrafted human hepatocytes without detectable liver fibrosis and inflammation. Moreover, human-specific sequencing reads in the ChIP-Seq pipeline are hepatocyte related because in liver bulk tissue only engrafted hepatocytes are of human origin. HCV-infected animals were cured using a combination of DAAs. Measurements of human albumin and HCV viral load in animals confirmed the viability of the engrafted hepatocytes and viral cure, respectively (Figure 5A). Similar to the findings in patients, we observed significant changes in H3K27ac levels in HCV-infected mice persisting after DAA cure (Figure 5B). Kyoto Encyclopedia of Genes and Genomes network analysis showed that pathways of genes showing epigenetic alterations included TNF signaling by nuclear factor κ B, IFN α/γ responses, complement, apoptosis, and mTOR signaling (Figure 5C). We found a persistence of TNF signaling through the nuclear factor κ B pathway, whereas the other HCV-induced pathways (ie, apoptosis, mTORC1 signaling, and IFN α/γ response) were restored to basal level after DAA-mediated cure (Figure 5C).

By intersecting genes associated with significant H3K27ac modifications from infected and cured mice, we identified 306 genes with persistent H3K27ac modifications after cure (Figure 5D and Supplementary Table 2). We found *SPHK1* and *KLF4* oncogenes and *SMO* TSGs, previously identified in patient samples (Figure 3C), to be associated with increased or decreased level of H3K27ac, respectively, in DAA-cured mice (Figure 5E), supporting the biological relevance of the findings in humanized mice. Similar to the results obtained in patients, we found a strong correlation between transcriptomic and epigenomic changes (Figure 5F).

Next, we identified HCV-specific epigenetic modifications in hepatocytes that are associated with HCC development by integrative analysis of epigenomic and transcriptomic data from patient and mouse liver samples. A comparative analysis of genes with persistent H3K27ac modifications in patients and mice showed a set of 65 commonly modified genes ($P = 2.94 \times 10^{-9}$; Figure 6A). Further analysis identified that some of these 65 genes have their transcripts significantly correlated to epigenetic changes after DAA cure in patients and humanized mice. We ranked their transcript expression based on the FC relative to the noninfected samples. This approach identified 38 genes that were enriched for H3K27ac and that are associated with a significant positive FC of their transcripts after HCV infection and DAA cure compared with noninfected samples (Figure 6B). We further studied the biological function of these 38 genes by performing gene set analysis and found that they are associated to KRas, TNF α , and interleukin 2 and signal transducer and activator of transcription 5 signaling or to p53, epithelial-mesenchymal transition, apoptosis, glycolysis, and inflammation pathways (Supplementary Figure 3). Because they were identified by integrative analysis of data from patients and immunodeficient humanized mice, we hypothesize that inflammation-related genes derive from the innate response of infected hepatocytes.

To obtain further evidence that these alterations play a role in hepatocarcinogenesis after cure, we compared their H3K27ac levels in paired liver tissues of nontumorous adjacent and HCC. We found that most of them already harbored changes in the nontumorous sample that remained in HCC tissue (Figure 6C). For instance, changes were observed for *SPHK1* in nontumorous tissue in 7 of 8 patients and persisted in HCC tissue in 4 patients. H3K27ac modifications in *SOX9*, a gene that is associated to ductular reaction, was found in nontumorous tissue in all DAA-cured patients and remained in HCC tissue in 7 of 8 patients.

HCV and Hepatocyte-Specific Epigenetic Modifications Translate Into Liver Protein Expression Changes and Are Associated With HCC Development in HCV Cirrhosis and SVR Cohorts

To further validate the biological relevance of HCV-induced epigenetic and transcriptional changes, we studied

Figure 5. Analysis of H3K27ac changes in livers of HCV-infected humanized mice identifies virus-specific modifications in human hepatocytes. (A) Our experimental setup: uPA-SCID mice were infected with HCV for 8 weeks and cured with a combination of DAAs MK7009 (50 or 100 mg/kg/d) and BMS-788329 (20 mg/kg/d) for 16 weeks. Livers were analyzed at week 24 by ChIP-Seq and RNA-Seq. Human albumin level (left) and HCV viral load (right) were measured to monitor functional engrafted human hepatocytes and HCV clearance after DAA treatment, respectively. (B) Unsupervised clustering of normalized read counts in ChIP-Seq peaks of 2483 genes linked with significant ($q < 0.05$) H3K27ac modifications in HCV-infected ($n = 5$) or DAA-cured ($n = 5$) vs noninfected control ($n = 5$) mice. (C) Hallmark pathways significantly enriched for H3K27ac modifications in infected ($n = 5$) or/and DAA-cured ($n = 5$) compared with noninfected ($n = 5$) mice samples. A significant overlap of enriched pathways persists in DAA-cured mice. (D) Venn diagram showing the HCV-induced and persistent genes with H3K27ac changes as the overlap of significantly modified genes in HCV-infected and DAA-cured mice derived from the ChIP-Seq experiment shown in B. (E) Oncogenes (red) and TSGs (green) with persistent HCV-induced H3K27ac modifications identified in the 306 HCV-induced and persistent genes with H3K27ac changes, with their biological functions indicated. (F) Heat map depicting transcriptional changes of the oncogenes and TSGs described in E in HCV-infected humanized and DAA-cured mice. EMT, epithelial-mesenchymal transition; NF κ B, nuclear factor κ B.

whether the expression of the identified genes correlates with corresponding protein abundance. We quantified the protein expression of *SPHK1* and *SOX9* genes by immunoblotting in patient and mouse liver samples (Figure 6D and E and Supplementary Figures 4–6). We found increased SPHK1 and SOX9 protein levels at HCV infection that remained increased after DAA cure. Importantly, by comparing pairwise liver tissue from adjacent nontumorous areas and HCC, we found that the expression of SPHK1 and SOX9 were already increased in adjacent nontumorous tissue (Figure 6D and E), suggesting that the up-regulation of these proteins preceded tumor development.

To assess the potential of the expression of these genes as biomarkers to predict HCC risk, we assessed the association of *SPHK1* expression with the long-term probability to develop HCC over a decade in a cohort of patients with HCV cirrhosis ($n = 216$), among which a subset of patients achieved SVR ($n = 21$). We found that high expression of *SPHK1* is significantly associated with HCC risk in the 2 cohorts ($P < .034$ for HCV cirrhosis and $P < .006$ for SVR; Figure 6F), identifying a potential predictor of HCC risk post SVR.

Discussion

Our study exposes a previously undiscovered paradigm showing that chronic HCV infection induces H3K27ac modifications that are associated with HCC risk and that persist after HCV cure. Thus far, only limited data have shown that HCV infection can induce epigenetic changes.²⁴ Previous attempts to connect specific histone marks to HCC development were inconclusive because of semi-quantitative approaches.^{25,26} For the first time, our study provides an integrative genome-wide approach that combines analyses in patient liver tissue and a humanized animal model.

Long-term epigenetic alterations also were observed after Epstein-Barr virus infection²⁷ or after transient hyperglycemia.²⁸ Indeed, latent Epstein-Barr infection triggered persistent epigenetic reprogramming, possibly resulting in the establishment of immortal growth and cancer, whereas transient hyperglycemia resulted in persistent enrichment of H3K4me1 on the *p65* gene

promoter and subsequently in oxidative stress and increased cancer risk. Importantly, these data suggest that persistent epigenetic changes also can occur through environmental changes, independently from direct viral infection.

Epigenetic changes in patient liver tissue can result from infected hepatocytes and from virus-induced inflammatory or fibrotic responses in the liver microenvironment. Interestingly, PCA showed a clear correlation of epigenetic changes with fibrosis stage (Figure 2A), suggesting that HCV-induced histone modifications and fibrogenesis are interdependent from the progression of liver disease. Indeed, epigenetic changes are considered as orchestrating fibrogenesis,²⁹ including the activation of hepatic stellate cells. In contrast, the induction of fibrosis triggers a liver response to injury, implicating the epigenetic machinery to mediate the activation of dedicated genes,³⁰ and thereby enhancing HCV-established epigenetic changes. Because distinct epigenetic changes were found in patient liver tissue and humanized mouse liver tissue (Figures 3 and 5), where no necro-inflammatory response or fibrosis is present, it is likely that a fraction of the observed changes is caused by direct HCV–hepatocyte interactions. Collectively, our results suggest that direct virus–hepatocyte interactions and indirect mechanisms, such as disease-induced fibrosis mediated by the liver non-parenchymal cells, contribute to the observed epigenetic changes in the livers of HCV-infected patients. Importantly, our data provide a previously undiscovered mechanism for persistent HCC risk after DAA cure in advanced fibrosis and could explain why a small number of patients develop HCC even in the absence of fibrosis.² However, we point out that this mechanism is not exclusive, and many other factors most likely contribute to hepatocarcinogenesis after cure.

Although we did not perform extensive functional studies, our data provide evidence that HCV-induced H3K27ac modifications on specific genes are causal factors for HCC risk after DAA cure. Our hypothesis is strongly supported by (1) altered expression of genes known to promote and drive carcinogenesis, (2) the correlation of epigenetic changes with a clinical Cox score for overall death and a HCC risk score,¹⁷ (3) the positive correlation between

Figure 6. Intersection of ChIP-Seq and RNA-Seq analyses from livers of patients and humanized mice uncovers HCV-induced persistent epigenetic changes associated with HCC risk after SVR. (A) Venn diagram showing the overlap of H3K27ac modifications between the human HCC risk gene candidates and significantly modified genes in HCV-infected and DAA-cured mice derived from the ChIP-Seq experiments shown in Figures 1B and 5B, respectively. (B) Expression data of genes with significant H3K27ac changes from livers of HCV-infected and DAA-cured patients ($n = 32$) and mice ($n = 15$) were intersected to uncover common genes with HCV-induced and persistent epigenetic and transcriptional changes after DAA. (C) Presence of epigenetic modifications on the 38 identified genes in pairwise liver tissues from DAA-cured patients. H3K27ac modifications (vs control liver samples) were assessed on the corresponding genes in nontumorous adjacent and HCC liver tissues from DAA-cured patients. *Dark blue squares* represent increased H3K27ac changes and *light blue squares* represent unchanged status. (D) Analysis of protein level of SPHK1 and SOX9 protein in control, HCV-infected, and DAA-cured mice by western blot. (E) Analysis of SPHK1 and SOX9 protein levels in control ($n = 7$), HCV-infected (non-HCC and HCC; $n = 8$) and DAA-cured (non-HCC and HCC; $n = 8$) patients by western blot. One representative gel of 4 is shown. Graphs show quantification of western blot intensities in arbitrary units normalized to total protein level (Ponceau staining). Results show mean \pm standard error of the mean of integrated blot densities. (F) Probability of HCC development according to the gene expression level of SPHK1 among 216 patients with HCV-induced cirrhosis or 21 patients with HCC occurrence after HCV cure.

the magnitude of epigenetic changes and fibrosis stage, which is the strongest clinical risk factor for HCC,⁶ and (4) the presence of H3K27ac modifications in HCC tumors of the same patients. Collectively, these findings suggest that epigenetic modifications precede hepatocarcinogenesis. Among the identified genes, functional knockout of *SOX9* has been reported to decrease liver cancer cell growth,³¹ and *SPHK1* deletion decreased diethyl-nitrosamine-induced liver cancer in mice,³² whereas ETS translocation variant 4 (*ETV4*) is up-regulated and is associated to HCC progression.³³ Importantly, extended analysis in additional cohorts showed that those genes that were epigenetically changed by HCV infection and that persisted after DAA cure predicted HCC risk in cohorts of patients with HCV cirrhosis and SVR (Figure 6C). Although we do not have experimental evidence that HCV-mediated modulation of *SPHK1* or *SOX9* gene expression is sufficient to promote cancer, our data combined with published knowledge on the role of these proteins in cancer biology^{31,32} nevertheless suggest that *SPHK1* and *SOX9*, among additional tumor-associated proteins, participate in HCV-induced HCC. This strongly supports the hypothesis that H3K27ac alterations of the identified genes precede HCC onset.

Other well-known causes for HCC development are chronic HBV infection and NASH.² Interestingly, we found that H3K27ac modifications also are present in these etiologies (Figures 1B and 2B). In-depth analyses including PCA (Figures 2A and Supplementary Figure 2) showed etiology-independent and etiology-specific epigenetic profiles in liver disease.

Because of the difficulty of obtaining liver tissue after HCV cure, which was available only for patients with concomitant HCC, the number of patient tissues is limited. Because it is impossible to obtain healthy liver tissue for ethical reasons, the control samples from patients with nonviral minimal liver disease or adjacent tissue from patients undergoing surgery for metastasis for colorectal cancer exhibited heterogeneity. Furthermore, the H3K27ac mark constitutes only a part of the epigenetic gene regulation program. Nevertheless, the robust results obtained by clustering and statistical analyses combined with consistent results from patients of different cohorts and clinical centers and confirmation of the key concept in humanized mouse engrafted with hepatocytes from the same donor and infected with the same viral inoculum allowed arresting conclusions.

HCC is often asymptomatic and thus remains undiagnosed until the late stage. Therefore, there is an urgent medical need for biomarkers to predict HCC risk. A large body of literature has shown the association between the human epigenome and cancer development.³⁴ In this study, showing that HCV induces persistent epigenetic alterations after DAA cure provides a unique opportunity to uncover novel biomarkers for HCC risk, that is, from plasma through the detection of epigenetic changes of histones bound to circulating DNA complexes. Furthermore, by uncovering virus-induced epigenetic changes as therapeutic targets, our findings offer novel perspectives for HCC prevention—a key unmet medical need.

Supplementary Material

Note: To access the supplementary material accompanying this article, visit the online version of *Gastroenterology* at www.gastrojournal.org, and at <https://doi.org/10.1053/j.gastro.2019.02.038>.

References

1. Ryerson AB, Ehemann CR, Altekruse SF, et al. Annual report to the nation on the status of cancer, 1975–2012, featuring the increasing incidence of liver cancer. *Cancer* 2016;122:1312–1337.
2. Fujiwara N, Friedman SL, Goossens N, Hoshida Y. Risk factors and prevention of hepatocellular carcinoma in the era of precision medicine. *J Hepatol* 2018;68:526–549.
3. Boldanova T, Suslov A, Heim MH, Necseulea A. Transcriptional response to hepatitis C virus infection and interferon-alpha treatment in the human liver. *EMBO Mol Med* 2017;9:816–834.
4. El-Serag HB, Kanwal F, Richardson P, Kramer J. Risk of hepatocellular carcinoma after sustained virological response in veterans with hepatitis C virus infection. *Hepatology* 2016;64:130–137.
5. Kanwal F, Kramer J, Asch SM, et al. Risk of hepatocellular cancer in HCV patients treated with direct-acting antiviral agents. *Gastroenterology* 2017;153:996–1005 e1.
6. van der Meer AJ, Feld JJ, Hofer H, et al. Risk of cirrhosis-related complications in patients with advanced fibrosis following hepatitis C virus eradication. *J Hepatol* 2017;66:485–493.
7. Sajankila SP, Manthena PV, Adhikari S, et al. Suppression of tumor suppressor *Tsc2* and DNA repair glycosylase *Nth1* during spontaneous liver tumorigenesis in Long-Evans Cinnamon rats. *Mol Cell Biochem* 2010;338:233–239.
8. Zhang Y, Liu T, Meyer CA, et al. Model-based analysis of ChIP-Seq (MACS). *Genome Biol* 2008;9:R137.
9. Nakagawa S, Wei L, Song WM, et al. Molecular liver cancer prevention in cirrhosis by organ transcriptome analysis and lysophosphatidic acid pathway inhibition. *Cancer Cell* 2016;30:879–890.
10. Hoshida Y, Villanueva A, Sangiovanni A, et al. Prognostic gene expression signature for patients with hepatitis C-related early-stage cirrhosis. *Gastroenterology* 2013;144:1024–1030.
11. Jones PA, Issa J-PJ, Baylin S. Targeting the cancer epigenome for therapy. *Nat Rev Genet* 2016;17:630.
12. Cai MY, Hou JH, Rao HL, et al. High expression of H3K27me3 in human hepatocellular carcinomas correlates closely with vascular invasion and predicts worse prognosis in patients. *Mol Med* 2011;17:12–20.
13. Uchida T, Hiraga N, Imamura M, et al. Elimination of HCV via a non-ISG-mediated mechanism by vaniprevir and BMS-788329 combination therapy in human hepatocyte chimeric mice. *Virus Res* 2016;213:62–68.
14. Schmidl C, Rendeiro AF, Sheffield NC, Bock C. ChIPmentation: fast, robust, low-input ChIP-seq for histones and transcription factors. *Nat Methods* 2015;12:963–965.

15. Harrow J, Denoeud F, Frankish A, et al. GENCODE: producing a reference annotation for ENCODE. *Genome Biol* 2006;7(Suppl 1):S41–S49.
16. Subramanian A, Tamayo P, Mootha VK, et al. Gene set enrichment analysis: a knowledge-based approach for interpreting genome-wide expression profiles. *Proc Natl Acad Sci U S A* 2005;102:15545–15550.
17. Hoshida Y, Villanueva A, Kobayashi M, et al. Gene expression in fixed tissues and outcome in hepatocellular carcinoma. *N Engl J Med* 2008;359:1995–2004.
18. Calo E, Wysocka J. Modification of enhancer chromatin: what, how, and why? *Mol Cell* 2013;49:825–837.
19. Rohrbach T, Maceyka M, Spiegel S. Sphingosine kinase and sphingosine-1-phosphate in liver pathobiology. *Crit Rev Biochem Mol Biol* 2017;52:543–553.
20. Cai H, Xie X, Ji L, et al. Sphingosine kinase 1: A novel independent prognosis biomarker in hepatocellular carcinoma. *Oncol Lett* 2017;13:2316–2322.
21. Van Renne N, Roca Suarez AA, Duong FHT, et al. miR-135a-5p-mediated downregulation of protein tyrosine phosphatase receptor delta is a candidate driver of HCV-associated hepatocarcinogenesis. *Gut* 2018;67:953–962.
22. King LY, Canasto-Chibuque C, Johnson KB, et al. A genomic and clinical prognostic index for hepatitis C-related early-stage cirrhosis that predicts clinical deterioration. *Gut* 2015;64:1296–1302.
23. Hanahan D, Weinberg RA. Hallmarks of cancer: the next generation. *Cell* 2011;144:646–674.
24. Okamoto Y, Shinjo K, Shimizu Y, et al. Hepatitis virus infection affects DNA methylation in mice with humanized livers. *Gastroenterology* 2014;146:562–572.
25. Hayashi A, Yamauchi N, Shibahara J, et al. Concurrent activation of acetylation and tri-methylation of H3K27 in a subset of hepatocellular carcinoma with aggressive behavior. *PLoS One* 2014;9:e91330.
26. Ruthenburg AJ, Allis CD, Wysocka J. Methylation of lysine 4 on histone H3: intricacy of writing and reading a single epigenetic mark. *Mol Cell* 2007;25:15–30.
27. Scott RS. Epstein-Barr virus: a master epigenetic manipulator. *Curr Opin Virol* 2017;26:74–80.
28. El-Osta A, Brasacchio D, Yao D, et al. Transient high glucose causes persistent epigenetic changes and altered gene expression during subsequent normoglycemia. *J Exp Med* 2008;205:2409–2417.
29. Moran-Salvador E, Mann J. Epigenetics and liver fibrosis. *Cell Mol Gastroenterol Hepatol* 2017;4:125–134.
30. Bae WK, Kang K, Yu JH, et al. The methyltransferases enhancer of zeste homolog (EZH) 1 and EZH2 control hepatocyte homeostasis and regeneration. *FASEB J* 2015;29:1653–1662.
31. Richtig G, Aigelsreiter A, Schwarzenbacher D, et al. SOX9 is a proliferation and stem cell factor in hepatocellular carcinoma and possess widespread prognostic significance in different cancer types. *PLoS One* 2017;12:e0187814.
32. Chen J, Qi Y, Zhao Y, et al. Deletion of sphingosine kinase 1 inhibits liver tumorigenesis in diethylnitrosamine-treated mice. *Oncotarget* 2018;9:15635–15649.
33. Kim E, Kim D, Lee J-S, et al. Capicua suppresses hepatocellular carcinoma progression by controlling the ETV4–MMP1 axis. *Hepatology* 2018;67:2287–2301.
34. Wilson CL, Mann DA, Borthwick LA. Epigenetic reprogramming in liver fibrosis and cancer. *Adv Drug Deliv Rev* 2017;121:124–132.

Author names in bold designate shared co-first authorship.

Received December 10, 2018. Accepted February 27, 2019.

Reprint requests

Address requests for reprints to: Thomas F. Baumert, MD, INSERM U1110, University of Strasbourg, 3 rue Koeberlé, F-67000 Strasbourg, France. e-mail: thomas.baumert@unistra.fr.

Acknowledgments

We acknowledge the Centre de Ressources Biologiques (Biological Resource Centre; Strasbourg, France) for the management of patient-derived liver tissues. We acknowledge the work of the IGBMC high-throughput sequencing facility and the Quantitative Genomics Facility at the Department of Biosystems Science and Engineering at the scientific central facilities of ETH Zurich. The IGBMC high-throughput sequencing facility is a member of the France Génomique consortium (ANR10-INBS-09-08). The laboratory of Irwin Davidson is an *équipe labellisée* of the Ligue Nationale contre le Cancer.

Author contributions: Thomas F. Baumert initiated and coordinated the study. Thomas F. Baumert, Nouridine Hamdane, Frank Jühling, Mirjam B. Zeisel, Yujin Hoshida, and Bryan C. Fuchs designed experiments and analyzed data. Nouridine Hamdane, Emilie Crouchet, Christine Thumann, Marine A. Oudot, Clara Ponsolles, Armando Andres Roca Suarez, and Shen Li performed experiments. Frank Jühling performed computational analyses. Nabeel Bardeesy contributed to the concept and approach of the study. Christian Schmid and Christoph Bock performed sequencing of ChIPmentation experiments. Irwin Davidson, Houssein El Saghire, Antonio Saviano, Naoto Fujiwara, Catherine Schuster, Atsushi Ono, and Yujin Hoshida analyzed data. Patrick Pessaux, Michio Imamura, Takuro Uchida, Hideki Ohdan, Hiroshi Aikata, Kazuaki Chayama, Tullio Piardi, Daniele Sommacale, François Habersetzer, Michel Doffoël, and Tujana Boldanova provided clinical liver tissue samples. Nouridine Hamdane, Frank Jühling, François H.T. Duong, Bryan C. Fuchs, Joachim Lupberger, Mirjam B. Zeisel, and Thomas F. Baumert wrote the manuscript.

Conflicts of interest

Authors declare no conflict of interest.

Funding

This work was supported by the ARC (Paris) and the Institut Hospitalo-Universitaire (Strasbourg; TheraHCC IHUARC IHU201301187 to Thomas F. Baumert), the Foundation of the University of Strasbourg and Roche Institute (HEPKIN to Thomas F. Baumert and Yujin Hoshida), the Agence Nationale de Recherches sur le Sida et les Hépatites Virales (2017/1633 to Thomas F. Baumert), the U.S. Department of Defense (W81XWH-16-1-0363 to Yujin Hoshida and Thomas F. Baumert), the Cancéropôle du Grand-Est (AAP Emergence 2017 to Joachim Lupberger), the National Institutes of Health (DK099558 to Yujin Hoshida), and the Research Program on Hepatitis from the Japan Agency for Medical Research and Development, AMED (17fk0210104h0001 to Kazuaki Chayama). This project has received funding from the European Union's Horizon 2020 research and innovation program under grant agreement 667273 (HEPCAR to Thomas F. Baumert and Joachim Lupberger). This project has received funding from the European Research Council under the European Union's Horizon 2020 Research and Innovation Program under grant 671231 (HEPCIR to Thomas F. Baumert and Yujin Hoshida). This work has been published under the framework of the LABEX ANR-10-LABX-0028_HEPSYS, and PLAN CANCER 2014–2019 and benefits from a funding from the state managed by the French National Research Agency as part of the Investments for the Future Program, the French National Cancer Institute, and INSERM.

Supplementary Methods

HCV Infection of Human Hepatocyte Chimeric Mouse and DAA Treatment

cDNA-uPA^{+/+}/SCID^{+/+} (uPA/SCID) mice were created and human hepatocytes were transplanted as described previously.¹ Mice were intravenously inoculated with serum samples containing 10⁵ HCV particles. The viremic serum was obtained from an HCV-infected (genotype 1b) DAA-naïve patient who provided written informed consent to participate in the study, according to the process approved by the ethical committee of the hospital and in accordance with the ethical guidelines of the 1975 Declaration of Helsinki. Blood sampling was done weekly, and serum samples were divided into small aliquots and stored in liquid nitrogen before measurement of HCV RNA. All animal protocols were performed in accordance with the Guide for the Care and Use of Laboratory Animals (<https://grants.nih.gov/grants/olaw/guide-for-the-care-and-use-of-laboratory-animals.pdf>). The experimental protocol was approved by the Ethics Review Committee for Animal Experimentation of the Graduate School of Biomedical Sciences at Hiroshima University (A14-195). Sixteen mice were divided into 3 groups: 6 mice were infected with HCV and treated with DAAs, 5 mice were infected with HCV but were not treated with DAAs, and 5 uninfected and untreated mice were used as controls. After the establishment of stable viremia, HCV-infected mice were treated with a combination of MK-7009 (vaniprevir; Merck Sharp & Dohme Corp, Kenilworth, NJ) and BMS-788329 (NS5A inhibitor; Bristol-Meyers Squibb, New York, NY) as described previously.² Elimination of HCV in 6 treated mice was confirmed by the absence of HCV viremia 12 weeks after cessation of therapy and by undetectable HCV RNA by reverse transcription-nested polymerase chain reaction from extracted liver tissue. Five viremic mice and 5 control mice were sacrificed at week 8. All liver samples were snap frozen and stored at -80°C before analysis.

Processing of Raw ChIPmentation Data

Reads were aligned to the human genome (hg19) using HISAT2³ reporting up to 100 alignments per read. Data from humanized mice were mapped similarly, but to an artificial genome consisting of all human (hg19) and mouse (mm10) chromosomes, and only reads mapping to human chromosomes were kept for further analysis. Sorting, indexing, and other basic operations on alignments were performed with samtools⁴ and intersections of annotations and peaks with alignments were performed using bedtools intersect.⁵ Peaks were called in uniquely mapped reads filtered for duplicates using MACS2⁶ in standard mode and with corresponding input sequence data. Only samples with at least 10,000 peaks were used for further analyses. Peaks within all samples were intersected and used for counting reads if they overlapped in at least 2 samples. Close peak regions with a maximal distance of 500 bp were merged. Read counts of genes were defined as the sum of all reads in peak

regions overlapping the gene body or the promoter region, that is, the region up to 1500 bp ahead of the transcription start site.

Processing of RNA-Seq Data

Raw reads of patient's samples had to be trimmed for primer and quality using cutadapt.⁷ Reads were mapped using HISAT2³ to the human genome hg19 (patients) or to hg19 and mm10 (humanized mice) as described earlier for raw ChIPmentation data. Reads were counted with htseq-count, and a differentially expression analysis was performed with DESeq2 applying GENCODE 19.⁸ Reads were taken from our RNA-Seq experiments as described earlier and from external sources: RNA-Seq from infected vs control patients was taken from the GEO dataset GSE84346 (low ISG samples).

Pathway Enrichment and Correlation Analyses

The full downstream ChIP-Seq analysis was based on read counts in ChIP-Seq peaks called as described earlier. Differentially modified genes (GENCODE 19 annotation) and log₂ FCs were identified using these peak read counts as input for edgeR.⁹ Pathway enrichment analyses were performed using local javaGSEA with all gene sets included in MSigDB 6.0.¹⁰ We used the pre-ranked version of javaGSEA and genes were ranked for *P* values of differential expression and modification analyses. Figures showing enriched pathways and gene sets, Spearman correlations, and oncogene log₂ FCs were drawn using ggplot2 and the R environment. Immune-related genes used for calculating correlations were selected from MSigDB by including only genes from pathways with the term "IMMUNE" in their title. Heat maps of gene expression and histone modifications were generated by applying the heatmap.2 function in combination with clustering through Spearman correlation included in the R package gplots. Gene network analysis was performed based on 3 MSigDB subsets: Hallmark gene sets, curated gene sets, and gene ontology gene sets. Genes were assigned with the hallmarks of cancer in case they were found in gene sets whose designation matches a corresponding term. Network figures were generated manually using Cytoscape.¹¹ Genes were defined as to be "connected to the PLS" in the case they shared at least 1 common pathway listed in MSigB 6.0 with at least 1 of the 32 PLS genes.

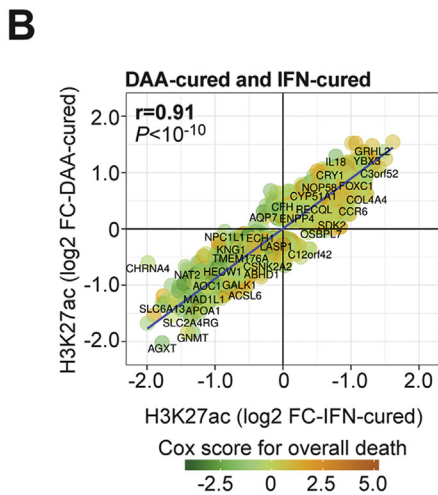
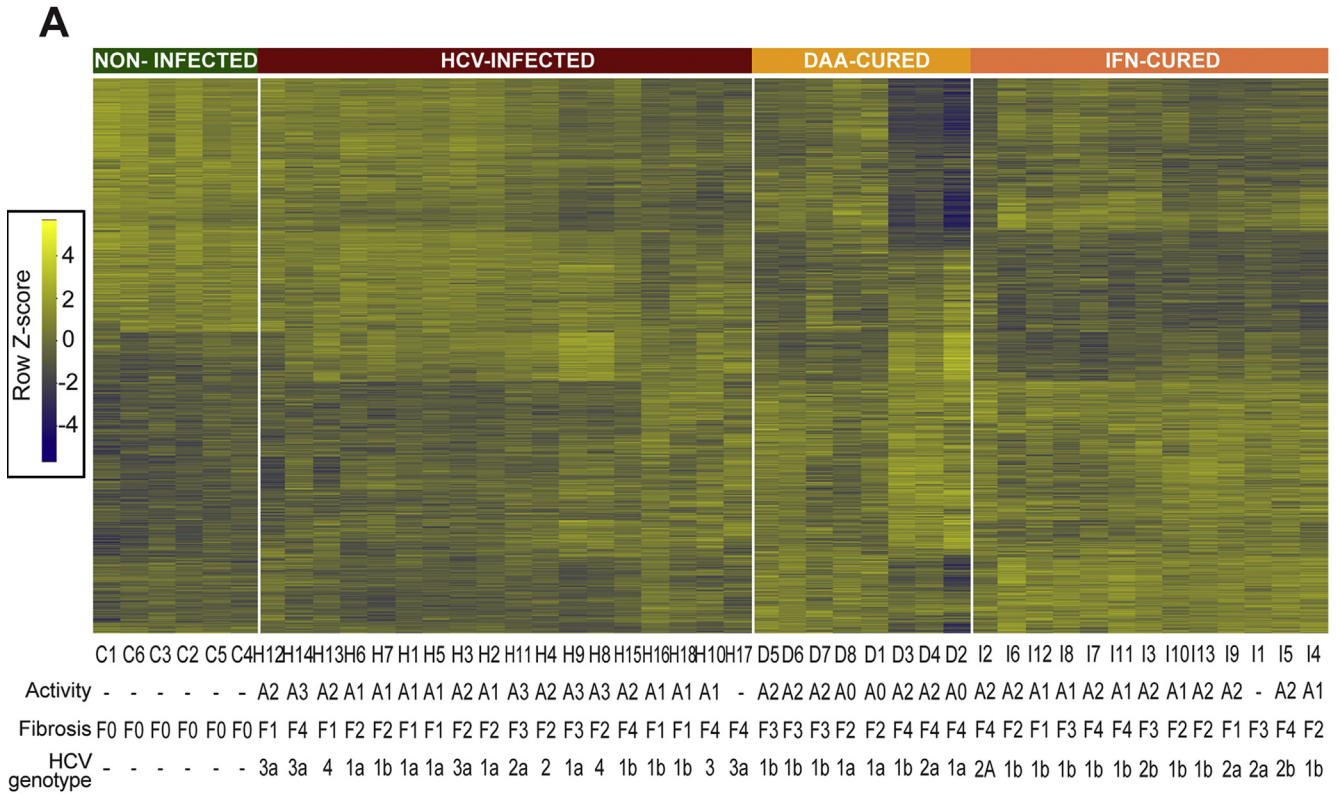
Western Blot and Antibodies

The expression of SPHK1 and SOX9 proteins was assessed by western blot using polyclonal rabbit antibodies anti-SPHK1 (D1H1L; number 12071) and anti-SOX9 (D8G8H; number 82630) from Cell Signaling (Danvers, MA). Protein expression was quantified using ImageJ software. Because anti-SPHK1 antibody detects all 3 isoforms¹² of SPHK1 and it is only partially understood which isoform or which post-translational modification on the oncogene SPHK1 predominantly triggers carcinogenesis, all apparent bands were included in the densitometry analysis.

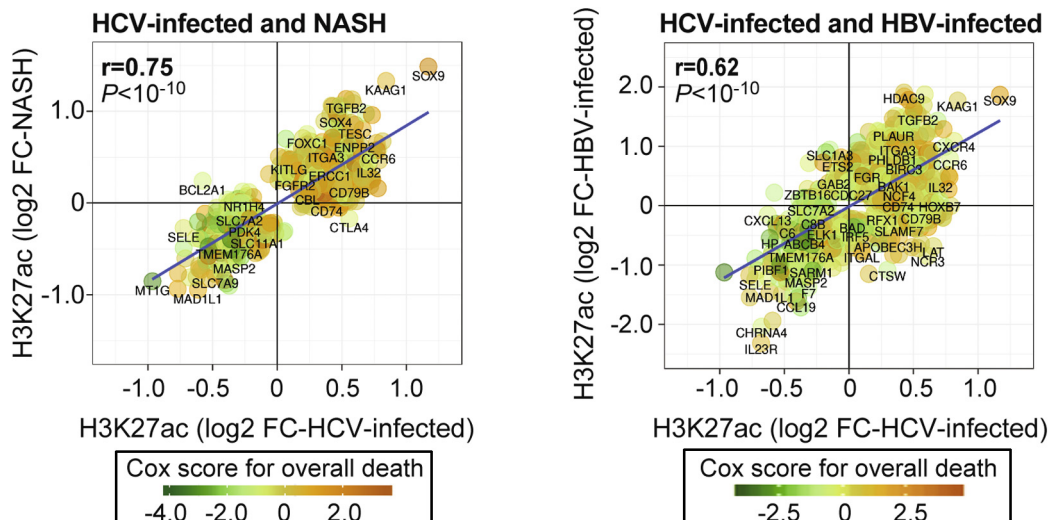
References

1. Tateno C, Kawase Y, Tobita Y, et al. Generation of novel chimeric mice with humanized livers by using hemizygous cDNA-uPA/SCID mice. *PLoS One* 2015; 10:e0142145.
2. Uchida T, Hiraga N, Imamura M, et al. Elimination of HCV via a non-ISG-mediated mechanism by vaniprevir and BMS-788329 combination therapy in human hepatocyte chimeric mice. *Virus Res* 2016; 213:62–68.
3. Kim D, Langmead B, Salzberg SL. HISAT: a fast spliced aligner with low memory requirements. *NatMethods* 2015;12:357–360.
4. Li H. A statistical framework for SNP calling, mutation discovery, association mapping and population genetic parameter estimation from sequencing data. *Bioinformatics* 2011;27:2987–2993.
5. Quinlan AR, Hall IM. BEDTools: a flexible suite of utilities for comparing genomic features. *Bioinformatics* 2010;26:841–842.
6. **Zhang Y, Liu T**, Meyer CA, et al. Model-based analysis of ChIP-Seq (MACS). *Genome Biol* 2008;9:R137.
7. Martin M. Cutadapt removes adapter sequences from high-throughput sequencing reads. *EMBnet.journal* 2011; <https://doi.org/10.14806/ej.17.1.200>.
8. **Harrow J, Denoeud F, Frankish A**, et al. GENCODE: producing a reference annotation for ENCODE. *Genome Biol* 2006;7(Suppl 1):S41–S49.
9. Robinson MD, McCarthy DJ, Smyth GK. edgeR: a Bioconductor package for differential expression analysis of digital gene expression data. *Bioinformatics* 2010;26:139–140.
10. **Subramanian A, Tamayo P**, Mootha VK, et al. Gene set enrichment analysis: a knowledge-based approach for interpreting genome-wide expression profiles. *Proc Natl Acad Sci U S A* 2005;102:15545–15550.
11. Shannon P, Markiel A, Ozier O, et al. Cytoscape: a software environment for integrated models of biomolecular interaction networks. *Genome Res* 2003;13:2498–2504.
12. **Hatoum D, Haddadi N**, Lin Y, et al. Mammalian sphingosine kinase (SphK) isoenzymes and isoform expression: challenges for SphK as an oncotarget. *Oncotarget* 2017;8:36898–36929.

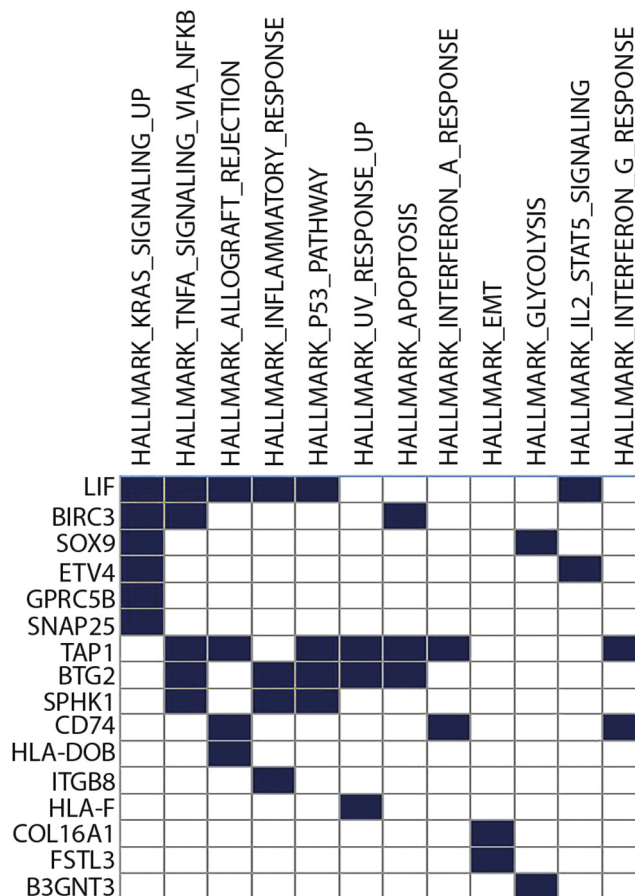
Author names in bold designate shared co-first authorship.



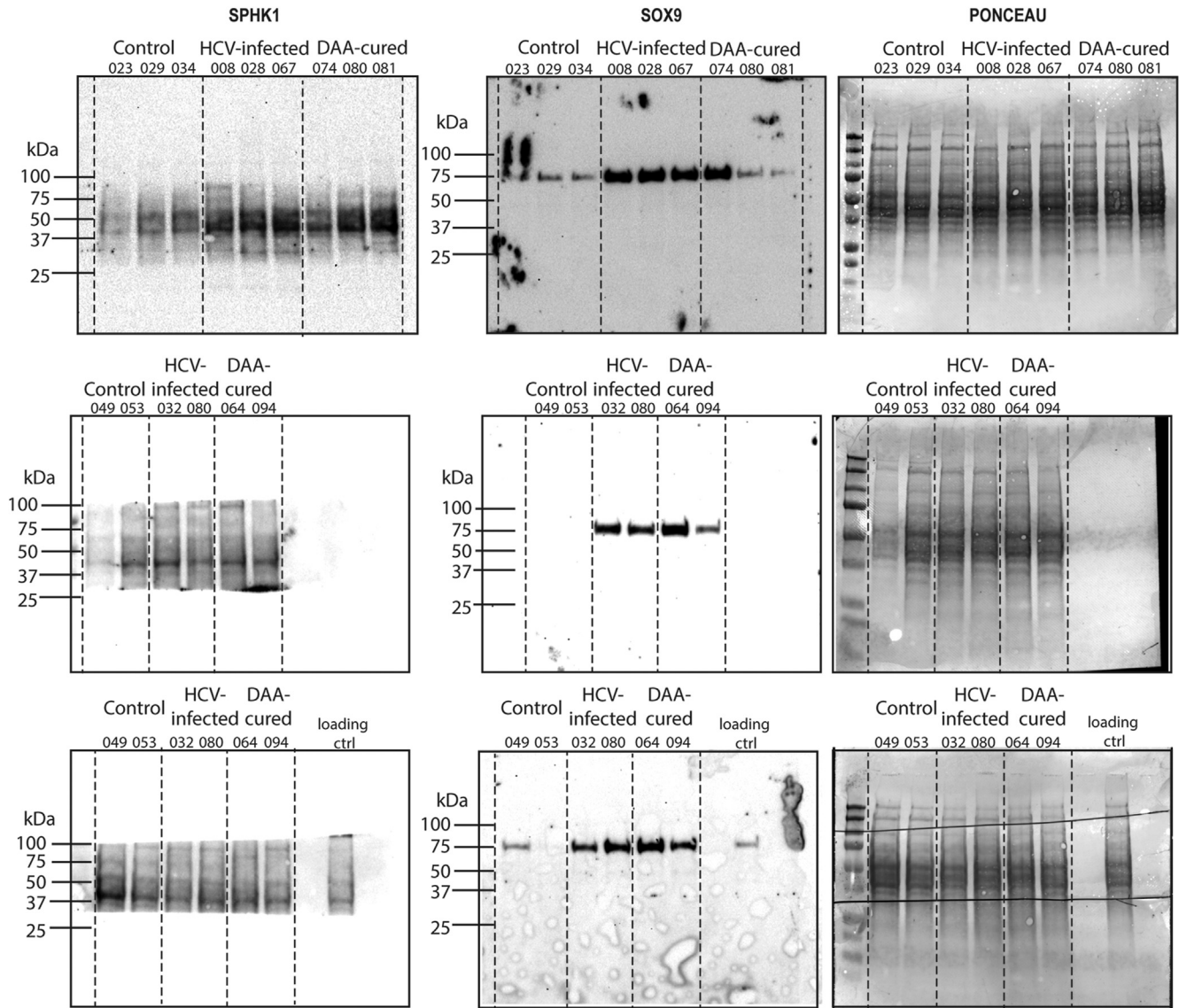
Supplementary Figure 1. Persistent H3K27ac modifications in the livers of DAA- and IFN-cured HCV-infected patients. (A) Unsupervised clustering of normalized read counts in ChIP-Seq peaks of genes linked with significant ($P < .05$) H3K27ac modifications in HCV-infected ($n = 18$), DAA-cured ($n = 8$), and IFN-cured ($n = 13$) vs noninfected control ($n = 6$) patients. (B) Persistent H3K27ac modifications among DAA-cured and IFN-cured patients correlate (see Spearman rank correlation coefficients r and P values) with H3K27ac modifications among IFN-cured patients.



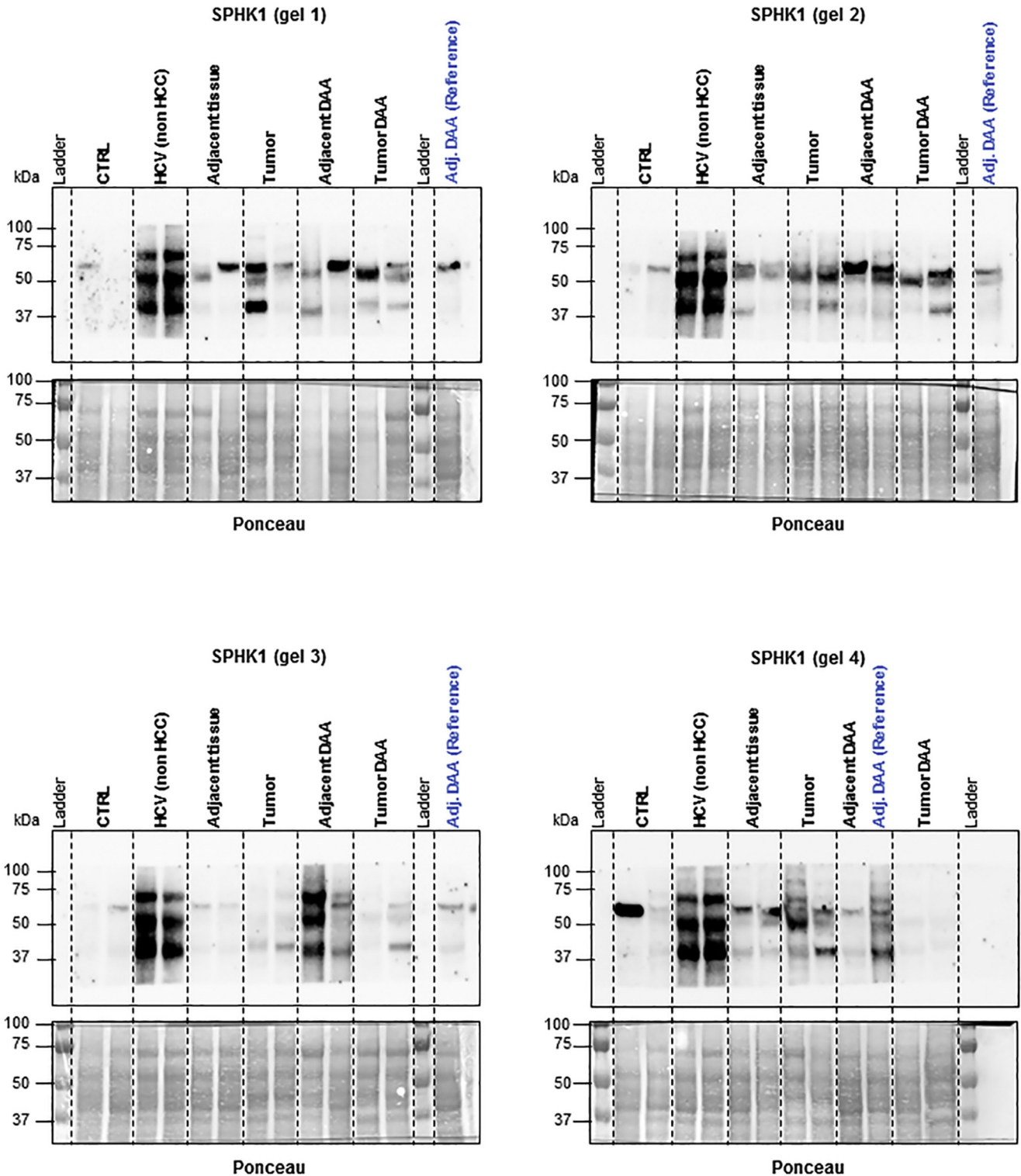
Supplementary Figure 2. Differential epigenetic modifications on immune-related gene signature among HCV-infected, NASH, and HBV-infected liver samples. To analyze the role of epigenetic changes in the disease immune responses, we extracted immune-related genes from MSigDB and performed a restricted correlation study of genes with H3K27ac modifications among NASH, HBV-infected, and HCV-infected patients. Common H3K27ac modifications were analyzed and Spearman rank correlation coefficients and *P* values are shown.



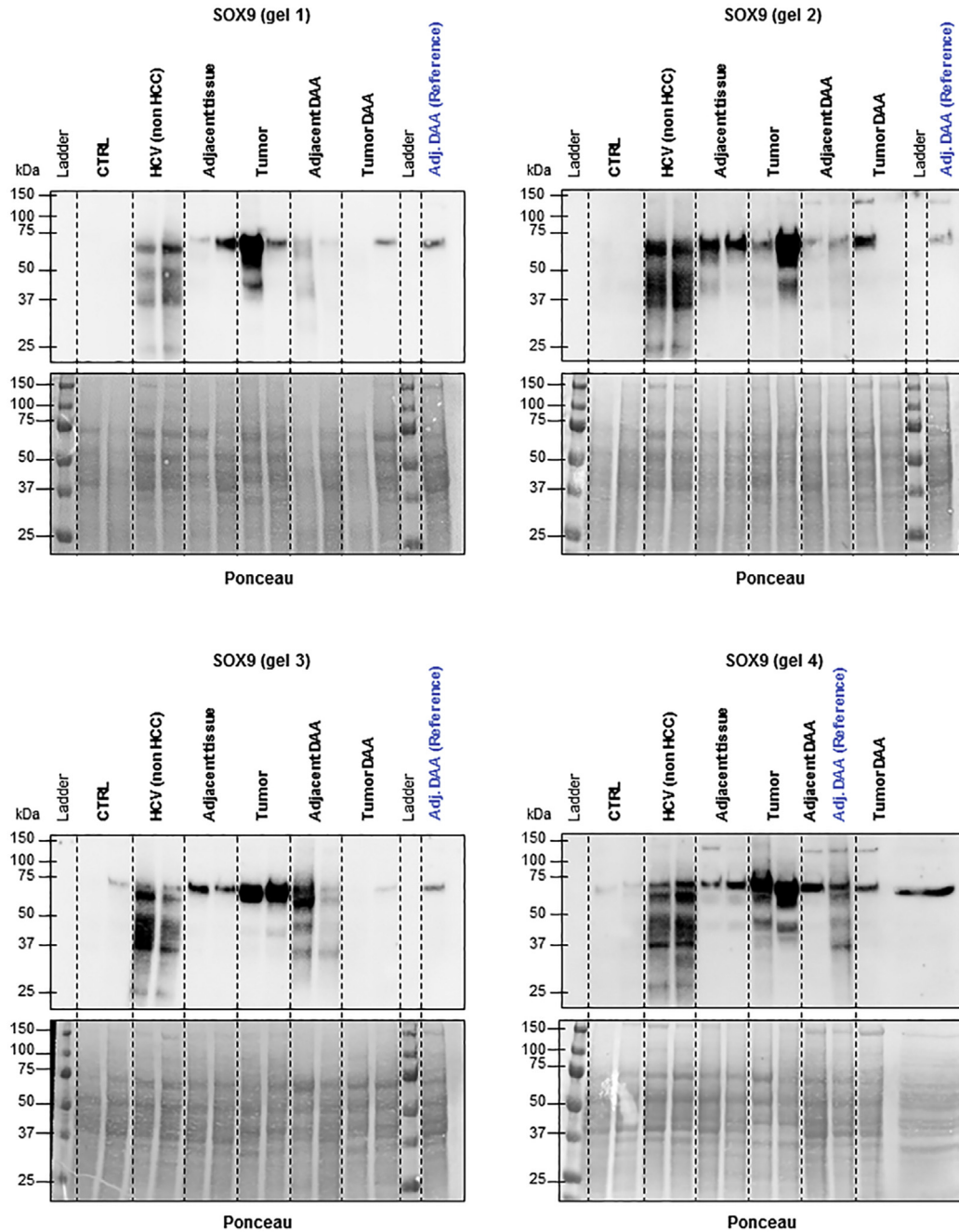
Supplementary Figure 3. Hallmark pathway analysis of the 35 genes enriched for H3K27ac modifications and overexpressed in infected and cured human ($n = 32$) and mice ($n = 15$) samples. The 38 genes harboring significant H3K27ac changes from the livers of HCV-infected and DAA-cured patients and mice were subjected to GSEA using hallmark gene sets from the MSigDB Molecular Signatures Database.



Supplementary Figure 4. Full-length immunoblots of SPHK1 and SOX9 protein levels in the livers of control, HCV-infected, and DAA-cured humanized mice. Full-length blots corresponding to representative blots shown in [Figure 6D](#) are shown. Reducing 10% sodium dodecyl sulfate–polyacrylamide gel electrophoresis of mouse liver lysates was performed as described in the Methods section.



Supplementary Figure 5. Full-length immunoblots of SPHK1 protein level in the livers of control, HCV-infected, and DAA-cured patients (HCC and adjacent tissue). For patients with HCC, SPHK1 was detected in tumor and surrounding tissues (adjacent tissue). A reference sample was loaded on each gel for data normalization. Full-length blots of SPHK1 corresponding to representative blots shown in [Figure 6E](#). Reducing 10% sodium dodecyl sulfate–polyacrylamide gel electrophoresis of liver biopsy lysates was performed as described in the Methods section. Multiple weight products visible on the blot could be a result of post-translational protein modifications including glycosylation, phosphorylation, and/or ubiquitination. CTRL, control.



Supplementary Figure 6. Full-length immunoblots of SOX9 protein levels in the livers of control, HCV-infected and DAA-cured patients (HCC or adjacent tissue). For patients with HCC, SOX9 was detected in tumor and surrounding tissues (adjacent tissue). A reference sample was loaded on each gel for data normalization. Full-length blots of SOX9 corresponding to representative blots shown in [Figure 6E](#). Reducing 10% sodium dodecyl sulfate–polyacrylamide gel electrophoresis of liver biopsy lysates was performed as described in the Methods section. Multiple weight products visible on the blot could be a result of post-translational protein modifications including glycosylation, phosphorylation, and/or ubiquitination. CTRL, control.